A Novel Integrated Biotrickling Filter -Anammox Bioreactor System for the Complete Treatment of Ammonia in Air with Nitrification and Denitrification

by

Lizhan Tang

Department of Civil & Environmental Engineering
Duke University

Date:_____

Approved:

_____
Marc Deshusses, Supervisor

_____
Mark Wiesner

_____
Claudia Gunsch

_____
Michael Bergin

Thesis submitted in partial fulfillment of
the requirements for the degree of
Master of Science in the Department of
Civil and Environmental Engineering in the Graduate School
of Duke University

2020

ABSTRACT

A Novel Integrated Biotrickling Filter -Anammox Bioreactor System for the Complete Treatment of Ammonia in Air with Nitrification and Denitrification

by

Lizhan Tang

Department of Civil and Environmental Engineering
Duke University

Date:_____

Approved:

_____
Marc Deshusses, Supervisor

_____
Mark Wiesner

_____
Claudia Gunsch

_____
Michael Bergin

An abstract of a thesis submitted in partial
fulfillment of the requirements for the degree
of Master of Science in the Department of
Civil and Environmental Engineering in the Graduate School of
Duke University

2020

Abstract

An integrated biotrickling filter (BTF)-Anammox bioreactor system was established for the complete treatment of ammonia. Shortcut nitrification process was successfully achieved in the biotrickling filter through free ammonia and free nitrous acid inhibition of nitrite oxidizing bacteria. During transients, while increasing nitrogen loading, free ammonia was the main factor that inhibited the activity of ammonia oxidizing bacteria (AOB) and nitrite oxidizing bacteria (NOB). During steady state operation, free nitrous acid was mainly responsible for inhibition of NOB due to the accumulation of nitrite at relatively low pH. Ammonia removal by the BTF reached up to 50 gN m^{-3} h^{-1} with 100% removal at an inlet concentration of 403 ppm and a gas residence time of 20.8 s. Average removal of ammonia during stable operation was 95%. The anammox bioreactor could remove 75% of total nitrogen discharged by the BTF when the two reactors were connected. The possibility of operating in complete closed loop mode for the liquid was investigated. However, due to the limited activity of the Anammox bioreactor or the fact that this reactor was undersized, recycling the Anammox effluent back to BTF caused accumulation of nitrite in the system which further inhibited activity of Anammox and progressively caused failure of the system.

A conceptual model of both bioreactors was also developed to optimize the integrated system. The model was developed by including mass balances of nitrogen in

the system and inhibition factors in microbial kinetics. Parameters such as hydraulic residence time (HRT), empty bed residence time (EBRT) and pH had significant impact on the partial nitritation process in the BTF. Model simulations also indicated that implementing a recycle for the Anammox bioreactor was needed to reduce the inhibitory effect of nitrite on the performance of the system.

Contents

List of Tables

List of Figures

Acknowledgement

I would like to thank my research supervisor, Dr. Marc Deshusses , for his patience on teaching me how to conduct an independent research. He was always willing to help me whenever I encountered difficulties in my scientific research. His expertise in the related field and kindness support contributed a lot to my achievement of this research project.

I also wanted to thank Lauren for recommending me into Dr. Deshusses lab and giving me the opportunity to study on what I really want to focus on. Thanks to Lauren's previous work, I obtained great experience establishing the integrated system.

Thanks the members of lab 024 and 027, especially Luis, Trisha, Kelsey and Jiyun, who helped me take care of my bioreactors when I was not in lab and gave me advice on how to conduct the experiment.

1. Introduction

1.1 Treatment of Ammonia Emissions in Air

Ammonia can be emitted from various sources such as fertilizer application, livestock raising, biomass burning and wastewater treatment plant operation (Behera, Sharma, Aneja, & Balasubramanian, 2013). Ammonia emissions can cause odor nuisances and affect human health. Ammonia emissions also have negative impacts on aquatic and terrestrial ecosystems due to deposition (Carfrae et al., 2004; Smith, Tilman, & Nekola, 1999). Conventional treatment of ammonia gas is generally through chemical scrubbing with acidic solutions. However, the costs of chemicals for scrubbing are large and absorbed ammonium in scrubbing liquid requires appropriate post treatment before discharging into aquatic system (Takeyuki Sakuma, Jinsiriwanit, Hattori, & Deshusses, 2008).

Biological treatment has become an effective alternative to conventional chemical scrubbing recently. Bioreactors such as biofilters and biotrickling filters are commonly applied in ammonia gas treatment (Deshusses, 2005; Kennes & Veiga, 2013). By inoculating nitrifying communities on packing materials, absorbed ammonia can be further nitrified to nitrite and nitrate which are suitable for disposal or post denitrification process. In traditional biofilters, ammonia is absorbed onto damp packing materials and then absorbed ammonia is available for further biotransformation. There are several studies demonstrating that biofilters can achieve high ammonia removal

efficiency (above 90% removal) with maximum inlet ammonia loading ranged from 4.5 gN m^{-3} h^{-1} to 22.5 gN m^{-3} h^{-1} (Baquerizo, Maestre, Machado, Gamisans, & Gabriel, 2009; Chen, Yin, & Wang, 2005; Kim, Rene, & Park, 2007). However, under medium or high loading conditions, biofilters usually accumulate free ammonia (FA) and free nitrous acid (FNA) in the damp volume of their packed beds, which can have an inhibitory effect on the activity of ammonia oxidizing bacteria (AOB) and nitrite oxidizing bacteria (NOB) and cause biofilter removal efficiency decrease (Baquerizo et al., 2005). Therefore, regular flushing and tight control of pH are needed to avoid failure of biofilters for long-term operation (Takeyuki Sakuma et al., 2008).

Compared to biofilters, biotrickling filters (BTFs) generally have greater elimination capacities due to the continuous trickling liquid that can lower the concentrations of FA and FNA accumulated inside reactors. Moreover, BTFs are more suitable for tight pH control through adding buffer solutions or acid-base solutions in liquid phase (Deshusses, 2005). The pH is usually an important factor that influences performance of BTFs as it influences the presence of ionized forms of accumulated metabolites. Although BTFs enable greater ammonia loading to be treated, BTF leachates will still contain high concentrations of nitrite and nitrate which can be problematic to dispose off because of their effects on aquatic environments. Thus, a subsequent denitrification process is desired to treat BTF leachate and reduce nitrogen liquid discharges. A handful of studies have been conducted to show the feasibility of such

combined processes. Sakuma et al. (2008) demonstrated that a biotrickling filter combined with a heterotrophic denitrification reactor can effectively remove ammonia gas with inlet loading up to 60 gN m^{-3} h^{-1}. With the denitrification reactor, the nitrate concentration in the system's effluent could be reduced close to zero. After treated by a post treatment reactor to remove excess COD, the effluent was recycled back to biotrickling filter which minimized water consumption for the whole process. Another study conducted by Raboni et al. (2016) illustrated that the performance of BTF could be improved through connecting with a denitrification reactor. The pH of the trickling liquid increased (as expected) from 7.3 to 8.0 after denitrification. Trickling liquid with a higher pH could be reused and provides autotrophic nitrifying bacteria with ideal condition to maintain optimal activity, since nitrification decreases the pH. Inhibitory effect by free nitrous acid was also diminished under alkaline condition.

To connect BTFs with conventional denitrification reactors, the ammonium present in aqueous phase must be mainly converted to nitrate, a process is commonly known as full nitrification. However, high nitrogen loading rate (NLR) can lead to accumulation of ammonium and nitrite in the liquid phase due to the fact that NOB are more susceptible to inhibitory effect than AOB (Baquerizo et al., 2005). Therefore, a greater rate of exchange is needed for the trickling liquid to lower the concentrations of metabolites and maintain full nitrification process.

Anammox –the anaerobic conversion of NO_2^- + NH_4^+ to nitrogen gas- has been increasingly applied in combination with partial nitritation ($NH_4^+ \rightarrow NO_2^-$) in the field of wastewater and landfill leachate treatment (Gut, Płaza, Trela, Hultman, & Bosander, 2006; Lackner et al., 2014; Wang et al., 2016). Compared to conventional denitrification, Anammox is more attractive with lower operation cost and higher nitrogen removal efficiency (Mulder, Van de Graaf, Robertson, & Kuenen, 1995). There is no literature reporting on BTF-anammox combination system for ammonia gas treatment. Baquerizo et al. (2017) proposed that through regulation of hydraulic residence time and nitrogen loading rate in a BTF, the ratio of NO_2^-N/NH_4^+-N in the effluent would be suitable for Anammox treatment. By applying Anammox process as an alternative to conventional denitrification process for post treatment, a BTF-anammox combination system can potentially minimize water consumption and electron donor consumption rates when treating air contaminated with ammonia. The reason is that such integrated system would allow for only partial inhibition of AOB activity but complete inhibition of NOB activity which means high concentrations of ammonium and nitrite can be maintained inside reactor without high rate of trickling liquid exchange. Moreover, operation conditions for biotrickling filter to achieve ideal partial nitritation have not been well studied yet.

1.2 Modeling of Integrated System

In previous studies, dynamic models of ammonia removal by biofilter filter and biotrickling filter have already been developed (Guillermo Baquerizo et al., 2005; T Sakuma, Aoki, Hattori, Gabriel, & Deshusses, 2004). Baquerizo et al. (2005) described the process of ammonia removal by a biofilter using a detailed model including FA and FNA inhibition in the microbial kinetic expressions. Sakuma et al. (2004) also developed a model of coupling of biotrickling filter and heterotrophic denitrification reactor to treat ammonia in air. Compared to Baquerizo et al, their simulation included mass balance for proton concentration to describe the dynamic change of pH in the system. Nevertheless, inlet concentration of ammonia was set very low (26 ppm) in simulation to achieve full nitrification. Both of these models primarily focused on the performance of the gas phase bioreactors instead of investigating the variations of concentrations of different nitrogen species in liquid phase. Partial nitritation (i.e., conversion of ammonium to nitrite only) process in BTF has not been specifically studied yet. Therefore, robust models that can describe performance of BTFs under medium or high ammonia load conditions need to be developed and a proper prediction of concentrations of the different nitrogen species in partial nitritation process is required.

There are few studies focusing on the modeling of specific Anammox biofilm reactors. Most of models present in these previous studies only focused on the kinetic model of anammox sludge in batch tests (Marina et al., 2016; Pradhan, Thi, & Wuertz,

2019; Tang, Zheng, Chai, & Min, 2013). Thus, a model to describe actual performance of Anammox reactors also needs to be developed to better understand potential operating conditions that may have impact on overall performance of an Anammox bioreactor.

Finally, to better understand how an integrated system with a BTF coupled with an Anammox bioreactor can best be integrated for effective ammonia treatment, the two models need to be combined and the entire system needs to be simulated. That will enable to understand the complex impacts of the many feedback loops that exist between the biological transformations between the two reactors. Thus, detailed models of a BTF and of an Anammox bioreactor were developed including inhibition coefficients in microbial kinetics, and they were then coupled. The models represented actual systems operated in the laboratory. In this coupled system, air contaminated with ammonia passed through the BTF and ammonia partitioned from the gas phase into trickling liquid and biofilm phases. Nitrifying communities grew on the packing material in the BTF in the form of a biofilm. Ammonia present in liquid phase diffused into biofilm where nitrification occurred. In the model, nitrification process was limited to its first step in which ammonia is only converted to nitrite by ammonia oxidizing bacteria (AOB) instead of more oxidized nitrate. Therefore, leachate of BTF contained high concentrations of ammonia and nitrite which is suitable for treatment by Anammox bioreactor. In the Anammox biofilm reactor, Anammox bacteria attached on carriers converted ammonia and nitrite to nitrogen under anaerobic condition.

1.3 Objective

The overall objective of this study was to study the feasibility of achieving long term partial nitritation of ammonia from air in a BTF and connecting it with an Anammox bioreactor for subsequent nitrogen removal and conversion to nitrogen gas at medium nitrogen loading condition. Supporting objectives to reach this goal was to investigate the mechanism of achieving partial nitritation in BTF and understand and quantify the inhibitory effects of FA and FNA. Additionally, to minimize water consumption of this integrated system, the potential of operating the system with the liquid in a closed loop will also be demonstrated.

A second focus of the work was on developing robust models for the integrated system. The mathematical models developed for this system were to help better understand inhibitory effect of FA and FNA on nitrifying communities and how partial nitritation of BTF can be achieved at steady state. The models also allow different parameters that may influence partial nitrtiation in the BTF to be investigated. The feasibility of connecting BTF with Anammox at different inlet ammonia concentrations will be evaluated based on model simulation.

This master thesis builds on the work of a former student Lauren Frei, whose master thesis defended in 2018 was titled Ammonia Gas Removal Using a Biotrickling Filter Coupled with an Anammox Bioreactor. In her work, Lauren focused on the operation conditions for the startup of the biotrickling filter and Anammox bioreactors

and the two reactors were operated separately, and not at steady state for most of her work. Definitive proof that the proposed system could be operated reliably over extended periods of time was not achieved. Lauren also developed a mathematical model of the systems but integration was not achieved.

2. Experimental Study of Biotrickling Filter Coupled with Anammox Bioreactor

2.1 Materials and Methods

2.1.1 Startup of Biotrickling Filter and Operating Conditions

The biotrickling filter consisted of a PVC column with a height of 1.52 m and an inner diameter of 0.12 m. The reactor was packed with polyurethane foam cubes and packing volume accounted for 80% of the total volume. BTF was inoculated with activated sludge from North Durham Water Reclamation Facility (Durham, NC). Inoculated sludge (1 L) with mineral medium (0.5 L, see compositions below) were circulated through BTF for 24 h with only air supply. After the recirculation, 162 ppm_v of humidified ammonia gas in air at a flow rate of 10 ml min^{-1} passed through BTF for 8 days. Mineral medium concurrently trickled down the reactor at a flow rate of 10 ml min^{-1} with a peristaltic pump. Desired concentration of synthetic gas was kept through regulation of an Alicat Scientific mass flow controller for ammonia and a flow meter (Dwyer, United States) for air. No active pH control was implemented during the whole operation period for BTF.

After 8 days of acclimation, nitrogen loading rate was gradually increased to enhance biomass growth. The operation conditions in each phase before connecting with anammox bioreactor are shown in Table. 1. The startup period of BTF took 4 months. During the startup period, inlet ammonia concentration ranged from 162 ppm_v to 549 ppm_v. With empty bed residence time (EBRT) ranged from 20.8 s to 72.8 s, the

corresponding nitrogen loading rate ranged from 5.6 gN m^{-3} h^{-1} to 50 gN m^{-3} h^{-1}. Flow rate of fresh trickling liquid was kept at 10 ml min^{-1} corresponding to a hydraulic residence time (HRT) of 29 h. On day 73, a recirculation line was added (see Figure 1) at a flow rate of 26 ml min^{-1} to further improve the nitrification process. On day 122, a leak was detected in the ammonia gas inlet tubing which meant the actual ammonia loading was significantly lower than experimental calculated. Thus, inlet nitrogen loading rate was reduced from 60 gN m^{-3} h^{-1} to 45 gN m^{-3} h^{-1} for recovery of BTF. Nitrogen loading rate was increased back to 50 gN m^{-3} h^{-1} on day 268 and the operating condition was kept stable from then on.

The mineral medium contained : 0.3 g L^{-1} KH_2PO_4, 0.05 g L^{-1} $MgSO_4$, 0.025 g L^{-1} $CaCl_2$, 0.3 g L^{-1} $NaHCO_3$, 1ml L^{-1} trace element I and 1ml L^{-1} trace element II. Trace element I contained: 3.57 g L^{-1} $FeCl_2 \cdot 4H_2O$ and 5 g L^{-1} EDTA-$Na_4 \cdot 4H_2O$. Trace element II contained : 0.014 g L^{-1} H_3BO_3, 0.99 g L^{-1} $MnCl_2 \cdot 4H_2O$, 0.24 g L^{-1} $CoCl_2 \cdot 6H_2O$, 0.21 g L^{-1} $ZnCl_2$, 0.19 g L^{-1} $NiCl_2 \cdot 6H_2O$, 0.17 g L^{-1} $CuCl_2 \cdot 2H_2O$, 0.22 g L^{-1} $NaMoO_4 \cdot 2H_2O$, 0.11 g L^{-1} $NaSeO_4 \cdot 10H_2O$, 5 g L^{-1} EDTA-$Na_4 \cdot 4H_2O$

Table 1: Experimental conditions for BTF operation.

Phase	Period (d)	HRT (h)	EBRT (s)	Inlet NH_3 (ppm)	NLR (g N m^{-3} h^{-1})
I	0~7	28.7	72.8	162	5.6
	7~18	28.7	72.8	233	8
	18~24	28.7	54.8	319	14.5
	24~31	28.7	54.8	478	21.9
II	31~37	28.7	43.6	549	31.3
	37~115	28.7	20.8	404	50
	115~122	28.7	17.4	404	60
III	122~264	28.7	20.8	364	45
IV,V	264~392	28.7	20.8	404	50

2.1.2 Startup of Anammox Bioreactor and Operating Conditions

The Anammox bioreactor was an upflow biofilm reactor consisting of two connected PVC columns with different inner diameters. The upper part of the reactor had an inner diameter of 0.2 m and a height of 0.5 m. The lower part of the reactor had an inner diameter of 0.1 m and height of 0.6 m. The reactor was inoculated with Anammox rings from a side stream deammonification process operating at South Durham Water Reclamation Facility (Durham, NC). This shortened the startup phase to only one month, which is relevant since Anammox bacteria are slow growing organisms. Anammox bioreactor was initiated after BTF had already been in stable operation in Phase IV. During the startup phase, the reactor was directly fed with diluted BTF effluent to have the Anammox bacteria adapt to new conditions. Anammox influent flow rate was 14.4 L d^{-1} corresponding to a HRT of 15.8 h for first the 10 days. Total nitrogen loading rate gradually increased from 0.16 kgN m^{-3} d^{-1} to 0.31 kgN m^{-3} d^{-1}

through increasing inlet ammonium and nitrite concentrations. The average total nitrogen removal efficiency was 91%. For next 14 days, nitrogen loading rate was further increased to 0.82 kgN m^{-3} d^{-1} through a step increment of influent flow rate from 14.4 L d^{-1} to 57.6 L d^{-1}. During this period, the average inlet ammonium and nitrite concentrations for Anammox reactor were 122 mg L^{-1} and 147 mg L^{-1} which corresponded to a 4 fold dilution of BTF effluent concentrations. Average total nitrogen removal efficiency was 81%.

2.1.3 Experimental Setup for the Integrated System and Standard Operating Condition

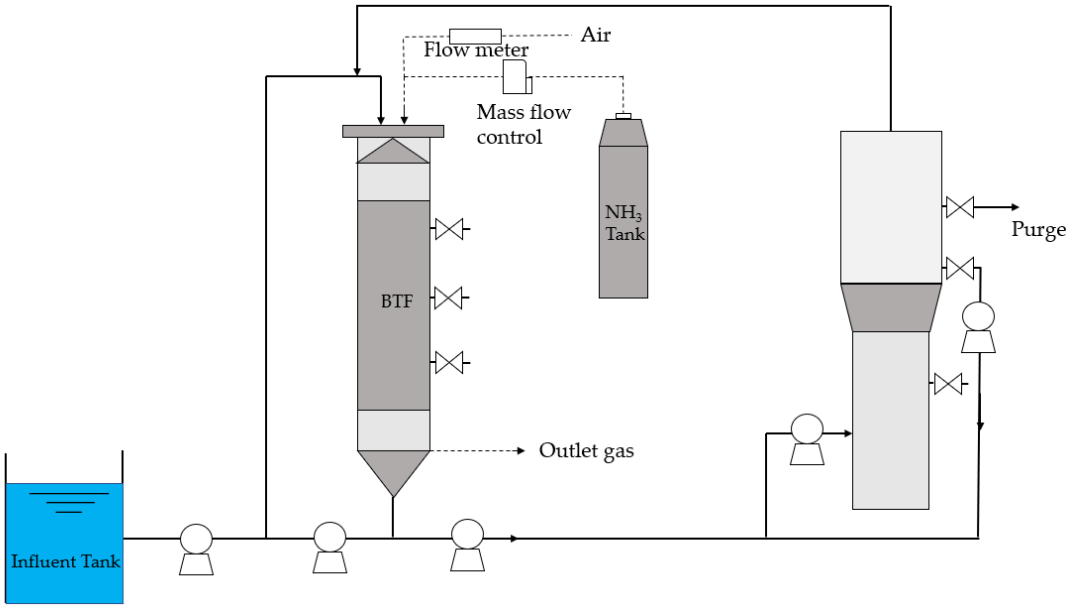

Figure 2: Schematic of the Experimental Setup.

After nitrogen removal rate (NRR) of Anammox reactor matched elimination capacity (EC) of BTF, the two reactors were connected. The experimental setup for the

integrated system was shown in Fig. 1. BTF effluent was directly fed into the Anammox bioreactor. Recirculation for the Anammox reactor was implemented to dilute inlet concentration.

For the integrated system, both BTF and Anammox inlet flow rates were 10 ml min^{-1}. Recirculation rates for BTF and Anammox were 26 ml min^{-1} and 30 ml min^{-1} respectively. 404 ppm_v of ammonia contaminated air passed through BTF with an EBRT of 20.8s. There were 3 phases for the operation of the integrated system. In Phase I and Phase II, BTF and Anammox bioreactor were connected in a one pass mode. The only difference between Phase I and II was the temperature for Anammox bioreactor. In phase I, Anammox reactor was operated at room temperature (22 C°-25 C°). In phase II, the temperature of Anammox bioreactor was kept between 28 C°-31 C° with heating tape in an attempt to increase treatment performance.

In phase III, the integrated system was operated in a (quasi) closed loop mode. Most of Anammox effluent was reused as trickling liquid for BTF. Due to the vaporization of water in the system, Anammox bioreactor effluent flow rate ranged from 11 L d^{-1}-13 L d^{-1}. 10 L of Anammox effluent was recycled back to BTF with 4.4 L fresh mineral medium every day. 1 L d^{-1} to 3 L d^{-1} purge was implemented to reduce accumulation of different nitrogen species (nitrite and nitrate) in the system.

2.1.4 Analytical Methods

Ammonia concentration in gas phase was monitored by TGS2602 gas sensor (Figaro，IL). Ammonium, nitrite and nitrate concentrations in liquid phase were measured using Hach Kits (AmVer High Range Ammonia Reagent Set for ammonium, Nitraver X reagent for nitrate and Spectroquant Nitrite Kit for nitrite). pH was monitored using LabQuest 2 monitor (Vernier, OR).

2.2 Results and Discussion

2.2.1 Overall Performance of the Biotrickling Filter

The overall performance of the BTF during the whole experimental period is shown in Fig. 2. Partial nitritation was successfully achieved during the whole period. Average nitrite accumulation ratio (NAR), defined as (nitrate nitrogen/nitrite nitrogen +nitrate nitrogen), in each phase was 84.9%±4.7%, 88.9%±4.7%, 90.7%±1.7%, 88.9%± 1.3% and 78.6%±6.7% respectively. While nitrate concentration remained low (27.8±17.9, 48.3±16.9, 46.8±7.8, 50.0±9.7 and 191.5±78.1 mg/L respectively). This suggest that the activity of NOB was inhibited to a large extent throughout the whole period. Slight decrease of NAR in phase V was due to the fact that effluent of Anammox bioreactor was recycled back to BTF resulting in accumulation of nitrate in the system. A review of the startup shows that for the first 5 days, BTF was operated at a low nitrogen loading of 5.6 gN $m^{-3}h^{-1}$. In this period, average ammonia removal efficiency was only 72.4%±5.7%

due to limited biomass growth and high pH. On day 8, the pH of biotrickling filter effluent decreased to 6.6 (Fig. 3c) which suggested that nitrification process was starting and that the production of H^+ caused a significant drop of pH. The ammonia gas removal efficiency increased to 100% because of improved nitrification. A quick step increase of nitrogen loading from 5.6 gN $m^{-3}h^{-1}$ to 21.9 m^{-3} h^{-1} was implemented to further improve biomass growth from day 8 to day 31. pH in the system during this period remained in the range of 6.15-6.6. Ammonia removal efficiency kept 94.3%±6.7% during this period. Nitrate concentration also slightly increased with increasing nitrogen loading in phase I. However, the quick step increment of nitrogen loading did not give NOB enough response time to adapt to new conditions with small amount of nitrate produced relative to nitrite.

In phase II, nitrogen loading rate was further increased from 21.9 gN m^{-3} h^{-1} to 50 gN m^{-3} h^{-1} with decreasing EBRT (to maintain the inlet gas concentration constant) in an attempt to increase performance to more industry relevant values. Due to the sharp rise of nitrogen loading and decrease in EBRT, average ammonia removal efficiency decreased significantly to 60.6%±9.9% during day 34-73. pH higher than 8.37 indicated that slow growing AOB was not able to respond to a sharp rise of nitrogen loading immediately. Thus, enough response time is needed to have the nitrification improved to balance pH increase due to ammonia absorption. A recirculation line for BTF was added on day 73 to further improve the nitrification process. After implementing

recirculation (day 73-day 115), pH began to drop due to the acclimation of AOB to the new conditions. Average ratio of total ammonia nitrogen (TAN) to total nitrite nitrogen (TNN) in liquid phase changed from 1.3 to 0.9 consistent with the acclimation of AOB explanation. The lower pH resulting from improved nitrification provided condition that favored ammonia absorption. Thus, an increase of ammonia removal efficiency to 83.1%±3.1% was observed. Nitrate concentrations in phase II did not increased significantly compared to phase I which indicated that growth of NOB was constantly inhibited (as desired to avoid nitrate) during this period.

An ammonia gas leak was detected at inlet port of BTF on day 122 after increasing NLR to 60 gN m^{-3} h^{-1}. Thus, the actual nitrogen loading was much lower than expected from day 122 to 125 with only around 100 mg/L of ammonium and nitrite present in the liquid phase. After the ammonia leak was fixed, NLR increased to 45 gN m^{-3} h^{-1} to have BTF recovered from the temporary destabilization. Slight increase of pH to 7.4 was observed for the first 3 days but quickly dropped below 7.0 after 8 days operation indicating that the AOB activity recovered. After the recovery, BTF was operated with a constant nitrogen loading rate of 45 gN m^{-3} h^{-1} and EBRT of 20.8 s in Phase III. The average ammonia removal efficiency and elimination capacity (EC) were 89.5%±5.3% and 40.3±2.4 gN m^{-3} h^{-1} respectively under stable operation. Nitrite accumulation ratio of 90.7%±1.7% indicated that stable partial nitritation was achieved under medium nitrogen load condition.

In phase IV, NLR increased from 45 gN m^{-3} h^{-1} to 50 gN m^{-3} h^{-1} (ammonia concentration was kept constant at 404 ppm). A sudden increase of pH was observed for the first 3 days. However, pH quickly dropped and nitrite concentrations increased which indicated that enriched biomass of AOB was able to respond to the increase of nitrogen loading within a short period of time. The average ammonia removal efficiency and elimination capacity were 94.7%±4.7% and 47.3±2.3 gN m^{-3} h^{-1} respectively. Average TAN / TNN ratio during day 286- day 310 reached 0.85 which was close to the stoichiometric ratio of Anammox reaction (0.76). Thus, the two reactors were connected on day 310. At that point, Anammox treatment rate was 0.57gN h^{-1} which was very close to the average nitrogen removal rate of the BTF (0.61 gN h^{-1}).

Phase V represented the condition that Anammox effluent was recycled as trickling liquid for BTF. Due to the limited nitrogen removal capacity of Anammox bioreactor compared to BTF, accumulation of different nitrogen species was observed in the system (see day 375 on Fig. 2b). However, the recycle did not have a large impact on the performance of BTF. Ammonia removal efficiency was still maintained at 93.7%±3.0 on average. This was probably due to the tolerance of AOB to the accumulation of metabolites, in particular nitrite, after the long term acclimation period. The impact of the accumulating nitrite on the Anammox reactor is discussed in Section 2.2.5.

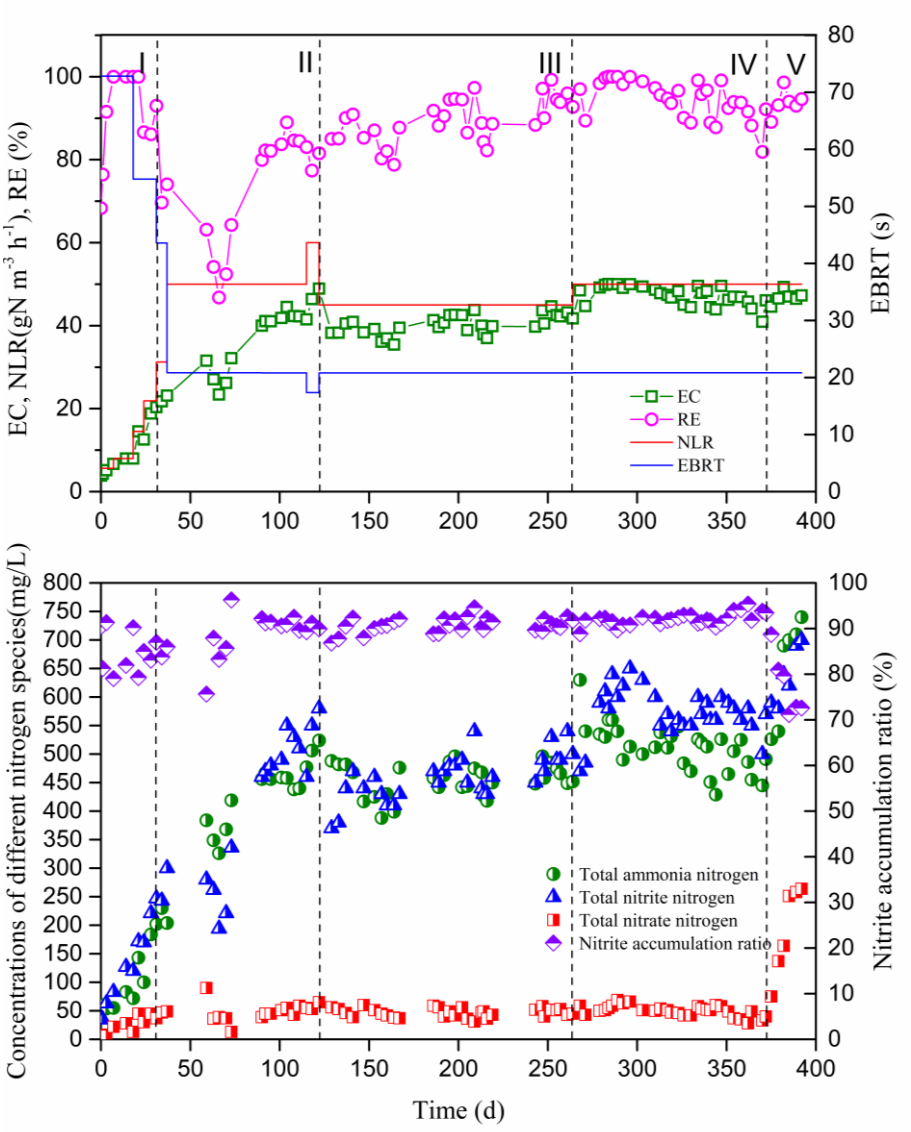

Figure 2: Biotrickling filter performance during the whole experimental period (a) gas phase (b) liquid phase. EC = elimination capacity. RE = removal percentage. NLR = nitrogen loading rate. EBRT = empty bed residence time.

2.2.2 Partial Nitritation in Biotrickling Filter

To deliver a feed with proper NH_4^+/NO_2^- ratio (0.76) to the Anammox bioreactor, achieving ideal partial nitritation in the BTF is crucial. It is generally considered that partial nitritation in a BTF can be achieved through inhibition of NOB by free ammonia

(FA) and free nitrous acid (FNA) accumulated in the system(Guillermo Baquerizo et al., 2005; Blázquez, Bezerra, Lafuente, & Gabriel, 2017). To understand how partial nitritation was achieved during the operation of the BTF in this study, the profile of concentrations of FA and FNA along vs. nitritation and nitratation rates were plotted and showed in Fig. 3. The concentrations of FA and FNA were calculated as below:

$$FA\left(\frac{mg}{L}\right) = \frac{17}{14} \times \frac{Total\ ammonia\ nitrogen\left(\frac{mg}{L}\right) \times 10^{pH}}{10^{pH} + e^{\frac{6344}{273+Temperature}}} \quad (1)$$

$$FNA\left(\frac{mg}{L}\right) = \frac{47}{14} \times \frac{Total\ nitrite\ nitrogen\left(\frac{mg}{L}\right)}{10^{pH} \cdot e^{\frac{-2300}{273+Temperature}}} \quad (2)$$

Nitritation rates and Nitratation rates were calculated as below:

$$Nitritation\ rates\ (gN\ m^{-3}\ h^{-1}) = EC + \frac{(C_{in,total\ ammonia\ nitrogen} - C_{out,total\ ammonia\ nitrogen})}{V} \cdot Q \quad (3)$$

$$Nitratation\ rates\ (gN\ m^{-3}\ h^{-1}) = \frac{(C_{out,total\ nitrate\ nitrogen} - C_{in,total\ nitrate\ nitrogen})}{V} \cdot Q \quad (4)$$

Where Q is the flow rate of trickling liquid ($m^3\ h^{-1}$), V is the volume of packed bed (m^3), EC is the elimination capacity ($gN\ m^3\ h^{-1}$), $C_{in,\ total\ ammonia\ nitrogen}$ is the concentration of total ammonia nitrogen in liquid influent, $C_{out,\ total\ ammonia\ nitrogen}$ is the concentration of total ammonia nitrogen in liquid effluent, $C_{in,\ total\ nitrate\ nitrogen}$ is the

concentration of total ammonia nitrogen in liquid influent, $C_{out,\ total\ nitrate\ nitrogen}$ is the concentration of total ammonia nitrogen in liquid effluent.

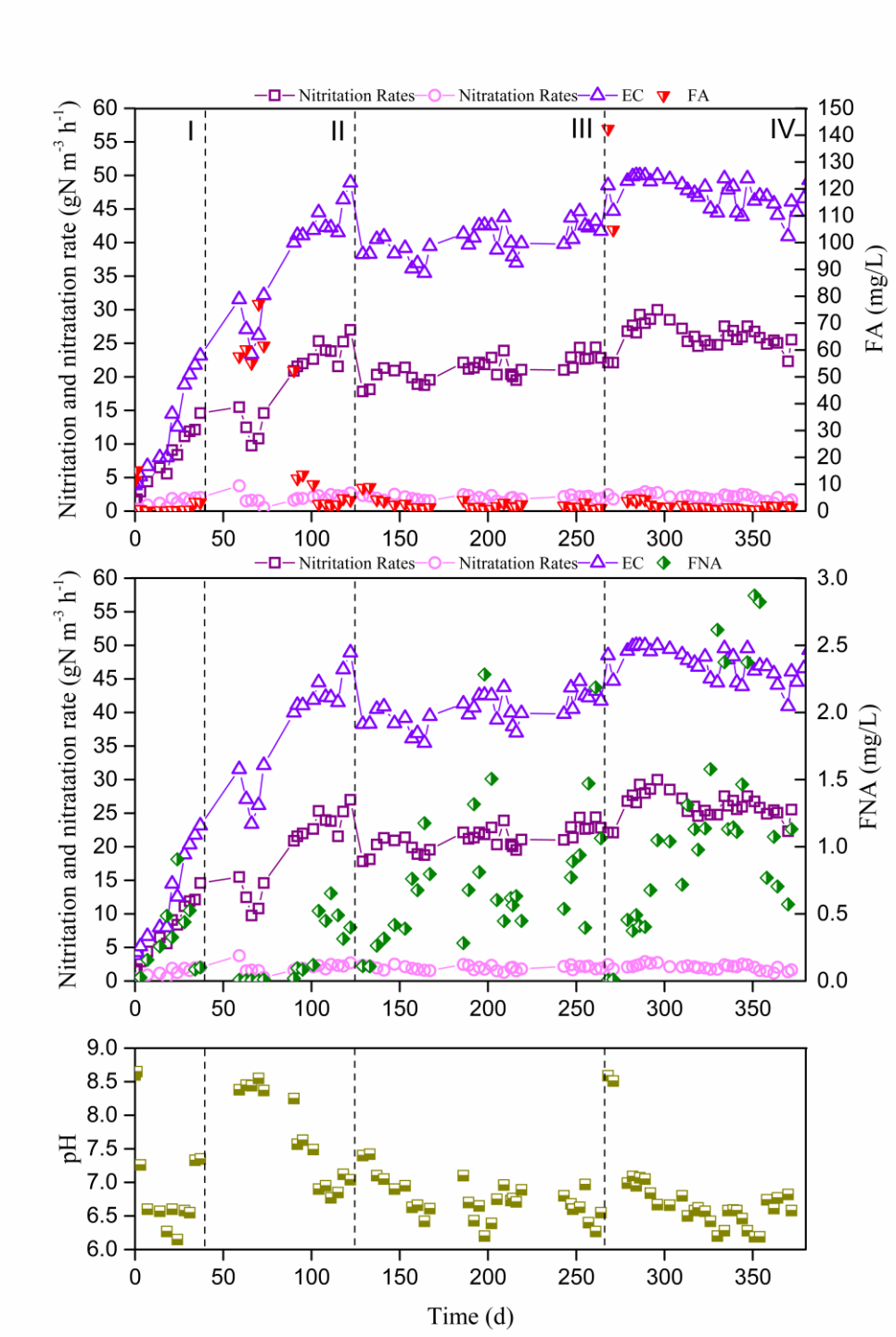

Figure 3: Variations of EC and nitrification rates (a) with free ammonia concentration (FA) (b) with free nitrous acid concentration (FNA) (c) variations of pH

The biotrickling filter in this study was started at a low nitrogen loading (5.6 gN m^{-3} h^{-1}) which is usually thought not to have inhibitory effect on nitrifying communities and full nitrification should be achieved under such condition according to studies conducted by other researchers(Blázquez et al., 2017; Takeyuki Sakuma et al., 2008). However, because in this study, the pH of biotrickling filter was not controlled, absorption of ammonia led to increase of pH that enabled high concentration of FA (9.6 mg/L-12.7 mg/L) present in liquid phase. FA concentration in this range did not cause inhibition of AOB but heavily suppressed the growth of NOB. Thus, significant increase of nitritation rates relative to nitratation rates was observed after 8 days of reactor initiation. There was study suggesting that inhibition of the growth of NOB starts at a FA level of 1.2 mg/L and complete inhibition on NOB occurrs at a FA level of 7.3 mg/L (V. Vadivelu, Keller, & Yuan, 2007). The activity of AOB, by comparison, was not inhibited at FA concentrations up to 85 mg/L (Hellinga, Van Loosdrecht, & Heijnen, 1999). The high pH along with selective inhibition of NOB by FA explained nitrite accumulation at such low nitrogen loading condition. With nitrification enhanced as a result of growth of AOB, pH began to drop. Therefore, inhibitory effect of FA was weakened with FA concentration dropping below 0.6 mg/L. A slight increase of nitratation rates was observed after day 8. However, due to the larger nitritation rates of AOB, level of nitrite in aqueous phase began to increase with increasing nitrogen

loading. Combined with a pH condition below 7, accumulated nitrite allowed for presence of FNA with an average concentration of 0.48±0.26 mg/L from day 14 - day 31. Nitratation rates did not increase during this period which strongly indicated that growth of NOB was inhibited. There were several studies reporting that activity of NOB is inhibited at FNA threshold ranged from 0.235 – 0.74 mg/L (Anthonisen, Loehr, Prakasam, & Srinath, 1976; Prakasam & Loehr, 1972). The biosynthesis (growth) of NOB can be even completely suppressed at a FNA concentration as low as 0.077 mg/L (V. M. Vadivelu, Yuan, Fux, & Keller, 2006).

In Phase II, a dramatic step increase of nitrogen loading from 31.3 gN m^{-3} h^{-1} to 50 gN m^{-3} h^{-1} led to the sudden increase of pH to 8.38. High concentration of FA （50.2±7.5 mg/L） at the high pH condition markedly inhibited the growth of NOB, and the activity of AOB was also temporarily suppressed at the high level of FA. Nitritation rates decreased from day 59 – day 73 because of the inhibitory effect of high concentration of FA on AOB. The average NH_4^+/NO_2^- ratio in effluent was 1.51±0.19 which also indicated a low conversion ratio of ammonium to nitrite. On day 73, a recirculation line was added to the BTF to further improve nitrification. After a long term acclimation of AOB to the high FA condition, pH began to drop and nitritation rates increased. Due to the decreased pH, inhibition of FA was weakened again and average NH_4^+/NO_2^- ratio decreased to 0.93±0.08. Stable pH ranged from 6.77 to 6.9 was obtained from day 104 to day 115 which suggested nitrification by AOB reached a

steady state. High concentration of FNA (0.49 mg/L – 0.71 mg/L) at this time suppressed growth of NOB constantly.

In Phase III and Phase IV which lasted a total of 273 days, BTF was operated with constant nitrogen loading of 45 gN m^{-3} h^{-1} and 50 gN m^{-3} h^{-1} respectively and reached steady state for most of the time. A steady-state pH was maintained below a value of 7 except during the transient stage from Phase III to Phase IV, where pH was temporarily high due to an increase of nitrogen loading. High concentration of FNA (0.92±0.56 mg/L for phase III and 1.31±0.80 mg/L for Phase IV) was mainly responsible for achieving stable partial nitritation in BTF at steady state operation. It should be noted that even under such high FNA level condition, there was still small amount of nitrate produced by NOB (46.8±7.8, 50.0±9.7 mg/L respectively). This indicated that although growth of NOB was largely inhibited, the energy generation process of NOB in the biofilm was still going on.

The experimental result of this study provided with a reliable way of achieving stable partial nitritation in BTF. During the startup phase (phase I and phase II), partial nitritation of BTF occurred, caused by alternating FA and FNA inhibition through the dynamic change of pH due to absorption of ammonia and nitrification process. At steady state, because of high concentration of accumulated nitrite and pH below 7, the presence of high level of FNA resulted in stable partial nitritation. It is worth mentioning that deficiency of alkalinity in the mineral medium relative to total ammonia nitrogen

loading was also partly responsible for the partial nitritation process. The ratio of alkalinity to total ammonia nitrogen in this study ranged from 0.2-1.8 mg $CaCO_3$/ 1mg TAN which was far less than the ratio of 7.14 mg $CaCO_3$/ 1mg TAN to achieve full nitrification (Li & Irvin, 2007). Meanwhile, the low alkalinity also allowed for the drop of pH below 7 through nitrification which was a suitable condition to maintain a high concentration of FNA essential for stable partial nitritation. Overall, these results show the many complex interdependencies between the activities of AOB and NOB, pH and concentrations of the different N species. Tight control of the conditions and a good understanding of these relationships are needed to successfully start and operate a BTF achieving partial nitritation.

2.2.4 Overall Performance of the Anammox Bioreactor

Fig. 4 shows the overall performance of the Anammox bioreactor for the 80 days operation of the experiment. Day 0 represents the first day that the Anammox bioreactor was connected to the BTF effluent. A recycle rate 3 times higher than the influent flow rate was implemented on the first day of connection to dilute inlet concentration and avoid substrate inhibition on Anammox. In Phase I, the reactor was operated at room temperature between 22 C°-25 C°. Average influent concentrations of ammonium and nitrite were 504±36 mg/L and 569±21 mg/L respectively. The average effluent concentrations of ammonium and nitrite were 130±32 mg/L and 39±12 mg/L,

corresponding to ammonium and nitrite removal efficiencies of 74.2%±6.5% and 93%± 2.2%, respectively. The large excess ammonium relative to nitrite in effluent was caused by the lower influent TNN/TAN ratio than the ratio of TNN/TAN consumed by Anammox. As shown in Fig. 4c, the influent TNN/TAN ratios through the whole operation period were lower than 1.32 which is theoretical stoichiometric ratio of Anammox process (Strous, Heijnen, Kuenen, & Jetten, 1998). It was suggested that a higher ratio of NO_2^--N/NH_4^+-N close to 1.32 can improve the nitrogen removal efficiency of Anammox with a constant loading (Tsushima, Ogasawara, Kindaichi, Satoh, & Okabe, 2007). Despite a larger amount of ammonium relative to nitrite in the influent, the concentration of nitrite did not decreased to zero which suggests that treatment capacity of the Anammox reactor did not fully match that of the BTF. In other words, a larger Anammox reactor or smaller BTF would have been needed.

The Anammox reactor temperature was increased to 30 C° in Phase II which was more suitable for Anammox growth to improve the treatment capacity of Anammox. A slight improvement of Anammox activity (4.8% increase) was observed in this phase. The average ammonium and nitrite removal efficiencies increased to 81.6%±2.4% and 96.4%±2.8% respectively. Between day 49 and day 51, the effluent nitrite concentration was below 5 mg/L. Total nitrogen removal rate reached 0.69 kgN m^{-3} d^{-1}. Higher temperature also reduced the concentration of FNA (by 12% from 25 °C to 30 °C) and therefore mitigated its inhibitory effect on Anammox activity (He et al., 2018).

A recycle at 10 L d^{-1} with 4.4 L d^{-1} mineral medium from Anammox bioreactor to BTF was implemented on day 62 to for the purpose of showing the ability of this system to operate with liquid in a quasi-closed loop. However, due to mismatch of the treatment capacity of Anammox reactor (0.56±0.03 mg h^{-1}) with that of BTF (0.89±0.13 mg h^{-1}), the influent nitrogen loading gradually increased in Phase III and greatly surpassed maximum nitrogen removal rate of Anammox reactor. Accumulation of nitrite and ammonium was observed in the system (see Day 59 in Fig.4). Anammox reactor performance was heavily impacted by the accumulation of substrates in the system. Average removal efficiency of ammonium and nitrite declined to 73.0%±7.3% and 80.1% ±9.5% respectively. In Phase III, the molar ratio of reacted NO_2^-/reacted NH_4^+ and produced NO_3^-/reacted NH_4^+ were below 1.32 and 0.26 respectively. This indicated that net growth of Anammox bacterium was inhibited to a large extent.

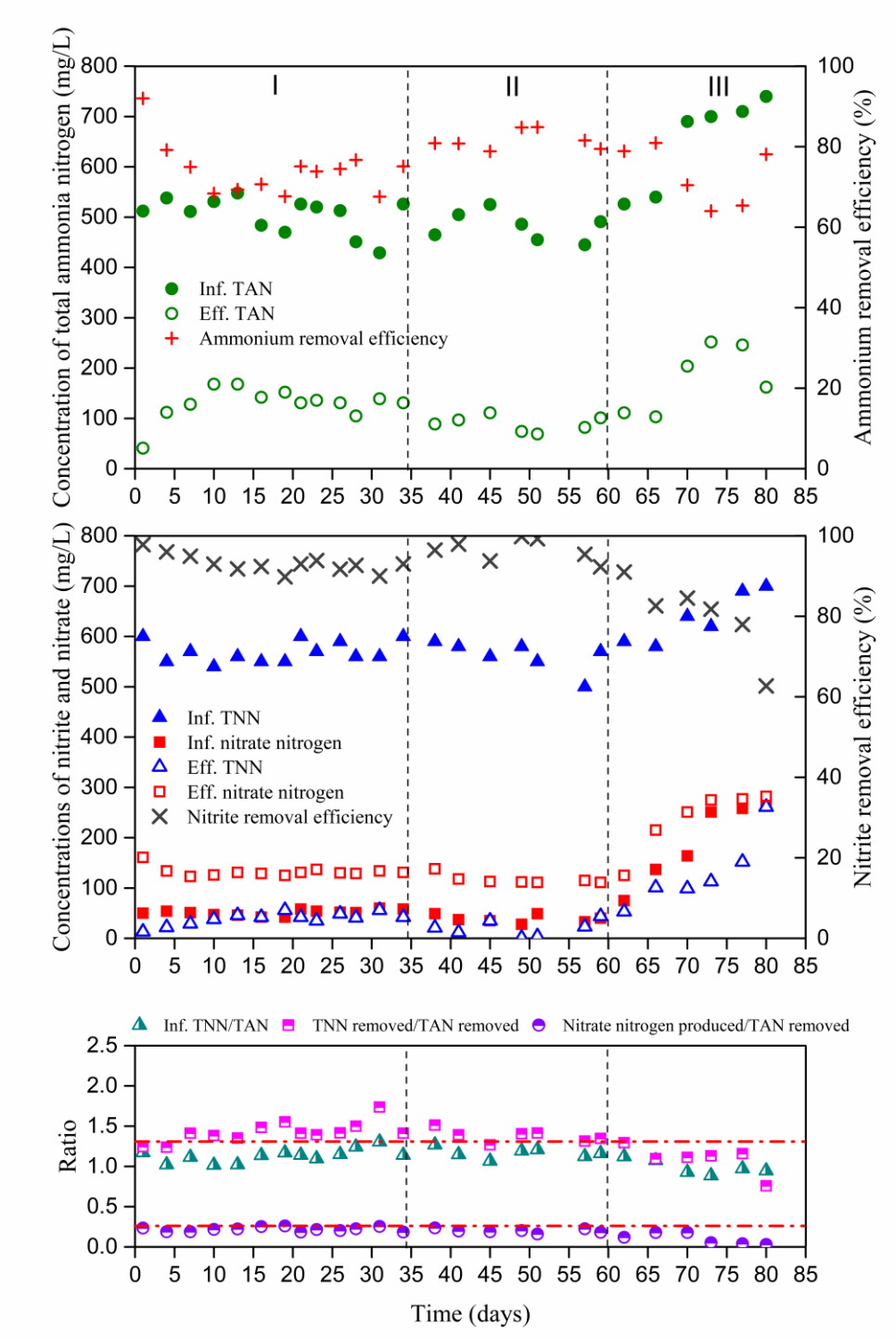

Figure 4: Performance of Anammox bioreactor after connecting with BTF. (a) concentration of TAN and ammonia removal efficiency (b) concentrations of TNN

and nitrate nitrogen and nitrite removal efficiency (c) ratio of ammonium, nitrite and nitrate

2.2.5 Effect of FA and FNA on Anammox Bioreactor

Accumulation of N species was the main reason that Anammox activity and performance got severely impaired and led to the slow failure of operating the system in a closed loop. Studies have shown that both high concentrations of ammonium and nitrite could inhibit Anammox activity whereas FA and FNA served as true inhibitors on Anammox process (Fernández et al., 2012; Hu, Zheng, Li, Xu, & Jin, 2006; Jin, Yang, Yu, & Zheng, 2012). To understand the effects of FA and FNA on Anammox bioreactor performance in this study, variations of FA and FNA during the operation period are shown in Fig. 4a. In phase I and phase II when the system was operated in one pass mode, concentration of FNA in Anammox effluent remained low (0.19 – 6.17 μg/L) because of high pH condition (7.7 – 8.48). In phase III when the system was operated in a closed loop, due to the accumulation of nitrite, FNA concentration increased significantly (25.2 – 180 μg/L). The activity of Anammox was gradually inhibited at such high level of FNA. Because of the suppression of Anammox activity, pH in Anammox reactor dropped from 8 to 7 （Fig. 4b） as a result of less alkalinity production by the denitrification process. The decrease in pH further inhibited the activity of Anammox and concentration of FNA continuously increased. Inhibition threshold of FNA ranged from 11 – 30.9 μg/L as reported by several studies ((Egli et al., 2001; Fernández et al., 2012; Isaka, Sumino, & Tsuneda, 2007). The concentrations observed were consistent

with previously published result. It should be noted that concentrations of FNA in our study were measured at the outlet port of the Anammox bioreactor. It is expected that concentration of FNA was higher at the inlet port (48.0 – 54.5 μg/L at pH of 7.4 in phase I, II and 56.4 – 111.4 μg/L at pH of 7.4 in phase III) due to a lower pH and higher concentration of total nitrite. However, other studies also showed that FNA concentration up to 60 μg/L did not have a significant inhibitory effect on Anammox activity (He et al., 2018). This was probably because for conventional upflow anaerobic sludge blanket bed (UASB), larger quantities of biomass were enriched at the inlet port of reactor which made them able to tolerate higher level of FNA at inlet port after a long term acclimation. In this study, FA concentration was always kept below 20 mg/L. No significant inhibitory effect of FA on Anammox was observed based on the result. Fernández et al. (2012) found that FA concentrations higher than 20-25 mg/L caused instabilities in their system. Tang et al. (2010) also reported that for an Anammox biofilm bioreactor, FA concentration of 57 – 178 mg/L had inhibitory effect on Anammox biofilm. Compared to FA, Anammox was more vulnerable to the inhibitory effect by FNA (Dapena-Mora et al., 2007). Therefore, accumulation of nitrite rather than ammonium was probably responsible for the failure of achieving long-term closed loop operation.

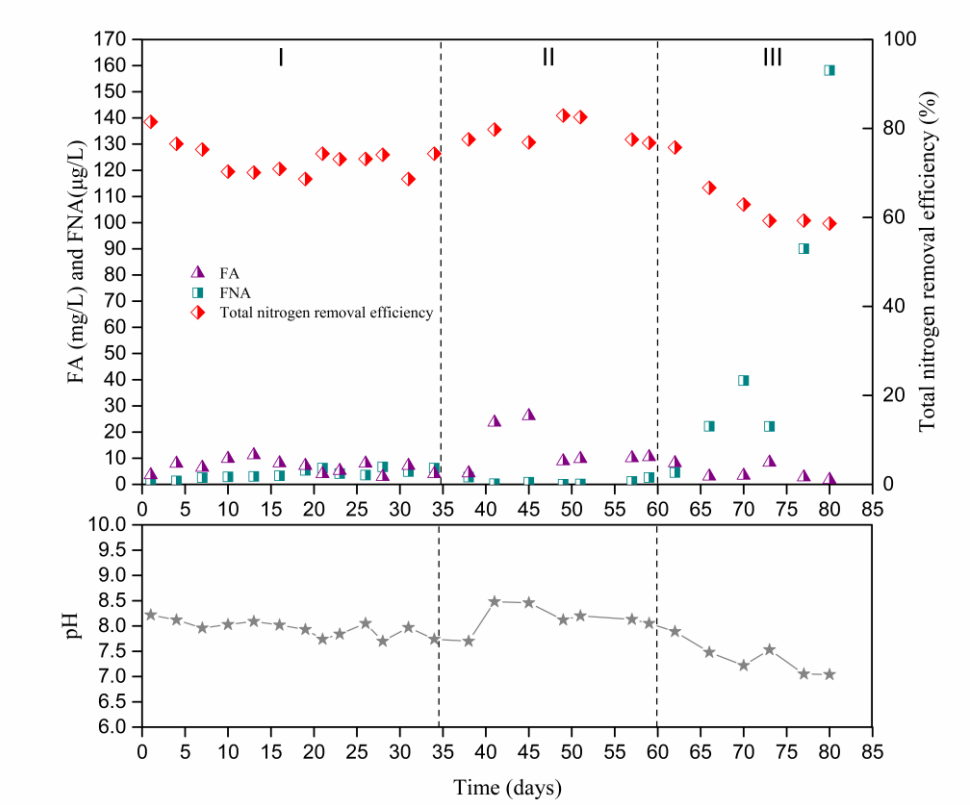

Figure 5: Variations of FA, FNA, TN removal and pH. (a) variations of FA, FNA, and TN removal (b) variations of pH

3. Modeling of Biotrickling Filter Coupled with Anammox Bioreactor

3.1 Model Description

Mathematical models were developed for the BTF and the Anammox bioreactors. The models aimed at being conceptually correct by discretizing space, transport and biotransformation phenomena as shown in Fig. 6. The general process of ammonia treatment by the integrated system was described by analyzing nitrogen mass balances for gas, liquid and biofilm phases. Each phase was discretized into several individual segments and mass balances for each individual segment were written. For the BTF, ammonia passed through the reactor and some portion of ammonia partitioned into the trickling liquid phase during contact between gas and liquid. Absorbed ammonia present in liquid phase was assumed to further diffuse into biofilm phase driven by concentration gradient which can be described by Fick's Law. Ammonia in biofilm phase was available for nitrification process in which ammonia was converted to nitrite first and then nitrate. Biotransformation of ammonia was described by microbial kinetic models for ammonia oxidizing bacteria and nitrite oxidizing bacteria including substrate inhibition factors. For Anammox bioreactor, the model was very similar in concept to that of the BTF. The only difference was that Anammox model did not have mass balance for gas phase and the kinetics were those of Anammox.

Several assumptions were made to simplify the models:

(1) Liquid and gas flow patterns for BTF and Anammox bioreactor follow plug flow behavior.

(2) Transfer of ammonia from gas phase into liquid phase follows the two-film theory and assumes equilibrium at gas-liquid interface.

(3) Transport of ammonia from liquid to biofilm is mainly through diffusion which can be described by Fick's law.

(4) There is no mass transfer resistance between biofilm and water phase.

(5) Biomass properties (thickness, specific area and microbial kinetics) are uniform along the reactor.

(6) Physical properties of biofilm are identical to those of water (diffusion coefficient, acid-base equilibrium coefficient).

(7) Biomass densities are constant and growth of biomass is neglected (considering nitrifying bacteria and anammox bacteria grow slowly).

(8) Biomass densities are uniform along the reactor (this assumption may not be correct due to concentration gradient of substrates along the reactor, the actual biomass densities along reactor need to be determined by actual experiments).

(9) Nitrification process is not limited by dissolved oxygen due to the fact that dissolved oxygen in actual experiments was in saturation.

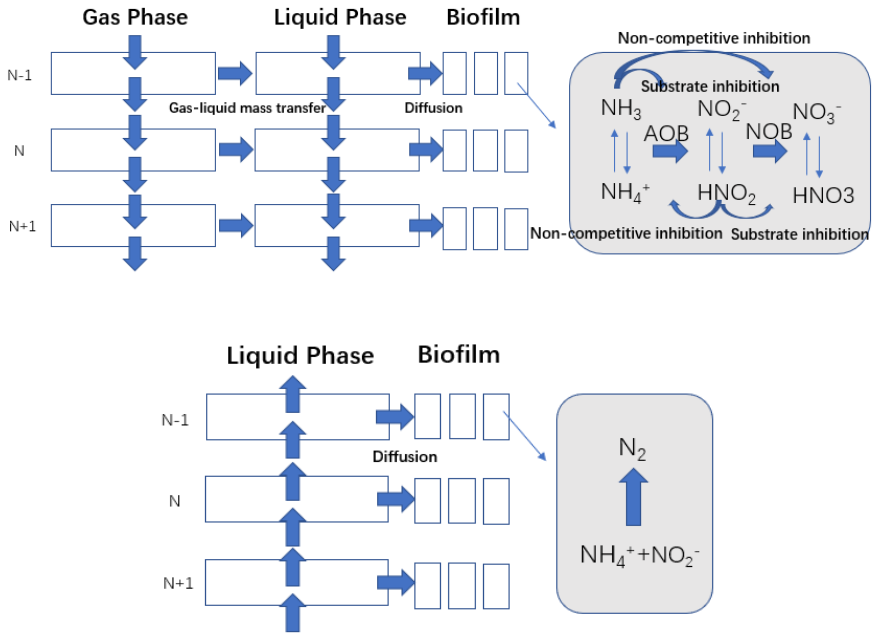

Figure 6: Conceptual Figure for the BTF and Anammox Bioreactor Models (a) BTF (b) Anammox bioreactor

3.2 Model Development

3.2.1 Biotrickling Filter Model Development

Mass balances for the gas phase:

$$\frac{dCg_{NH3}[1]}{dt} = \frac{G}{V_N \cdot e} \cdot \left(Cg_{NH3in} - Cg_{NH3}[1]\right) - k_g \cdot \frac{a}{e} \cdot \left(Cg_{NH3}[1] - \frac{Cl_{NH3}[1]}{kH}\right)$$

$$\frac{dCg_{NH3}[1..N]}{dt} = \frac{G}{V_N \cdot e} \cdot \left(Cg_{NH3in} - Cg_{NH3}[i]\right) - k_g \cdot \frac{a}{e} \cdot \left(Cg_{NH3}[1] - \frac{Cl_{NH3}[i]}{kH}\right)$$

Where G is the gas flow rate ($m^3\ d^{-1}$), V_N is the volume for one individual horizontal layer (m^3), k_g is the (gas film) mass transfer coefficient for ammonia ($m\ d^{-1}$), kH is the

Henry's law constant for ammonia, *e* is the porosity of BTF, a is the biofilm specific surface area (m^{-1}).

Mass balances for the liquid phase:

$$\frac{dCl_{NH3}[1]}{dt} = \frac{F}{V_N \cdot hc} \cdot (Cl_{NH3in} - Cl_{NH3}[1]) - k_g \cdot \frac{a}{hc} \cdot \left(Cg_{NH3}[1] - \frac{Cl_{NH3}[1]}{kH}\right) - \frac{D1 \cdot a}{hc \cdot \delta} \cdot (Cl_{NH3}[1] - Cb_{NH3}[1,j]) + r_{eq,NH3}[1]$$

$$\frac{dCl_{NH3}[1..N]}{dt} = \frac{F}{V_N \cdot hc} \cdot (Cl_{NH3in} - Cl_{NH3}[i]) - k_g \cdot \frac{a}{hc} \cdot \left(Cg_{NH3}[i] - \frac{Cl_{NH3}[i]}{kH}\right) - \frac{D1 \cdot a}{hc \cdot \delta} \cdot (Cl_{NH3}[i] - Cb_{NH3}[i,j]) + r_{eq,NH3}[i]$$

$$\frac{dCl_{NH4}[1]}{dt} = \frac{F}{V_N \cdot hc} \cdot (Cl_{NH4in} - Cl_{NH4}[1]) - \frac{D1 \cdot a}{hc \cdot \delta} \cdot (Cl_{NH4}[1] - Cb_{NH4}[1,j]) + r_{eq,NH4}[1]$$

$$\frac{dCl_{NH4}[1..N]}{dt} = \frac{F}{V_N \cdot hc} \cdot (Cl_{NH4in} - Cl_{NH4}[i]) - \frac{D1 \cdot a}{hc \cdot \delta} \cdot (Cl_{NH4}[i] - Cb_{NH4}[i,j]) + r_{eq,NH4}[i]$$

$$\frac{dCl_{NO2}[1]}{dt} = \frac{F}{V_N \cdot hc} \cdot (Cl_{NO2in} - Cl_{NO2}[1]) - \frac{D2 \cdot a}{hc \cdot \delta} \cdot (Cl_{NO2}[1] - Cb_{NO2}[1,j]) + r_{eq,NO2}[1]$$

$$\frac{dCl_{NO2}[1..N]}{dt} = \frac{F}{V_N \cdot hc} \cdot (Cl_{NO2in} - Cl_{NO2}[i]) - \frac{D2 \cdot a}{hc \cdot \delta} \cdot (Cl_{NO2}[i] - Cb_{NO2}[i,j]) + r_{eq,NO2}[i]$$

$$\frac{dCl_{HNO2}[1]}{dt} = \frac{F}{V_N \cdot hc} \cdot (Cl_{HNO2in} - Cl_{HNO2}[1]) - \frac{D2 \cdot a}{hc \cdot \delta} \cdot (Cl_{HNO2}[1] - Cb_{HNO2}[1,j]) + r_{eq,HNO2}[1]$$

$$\frac{dCl_{HNO2}[1..N]}{dt} = \frac{F}{V_N \cdot hc} \cdot (Cl_{HNO2in} - Cl_{HNO2}[i]) - \frac{D2 \cdot a}{hc \cdot \delta} \cdot (Cl_{HNO2}[i] - Cb_{HNO2}[i,j]) + r_{eq,HNO2}[i]$$

$$\frac{dCl_{NO3}[1]}{dt} = \frac{F}{V_N \cdot hc} \cdot (Cl_{NO3in} - Cl_{NO3}[1]) - \frac{D3 \cdot a}{hc \cdot \delta} \cdot (Cl_{NO3}[1] - Cb_{NO3}[1,j]) + r_{eq,NO3}[1]$$

$$\frac{dCl_{NO3}[1..N]}{dt} = \frac{F}{V_N \cdot hc} \cdot (Cl_{NO3in} - Cl_{NO3}[i]) - \frac{D3 \cdot a}{hc \cdot \delta} \cdot (Cl_{NO3}[i] - Cb_{NO3}[i,j]) + r_{eq,NO3}[i]$$

Where *hc* is the dynamic holdup for trickling liquid, *F* is the flow rate of liquid ($m^3\ d^{-1}$), *D1*, *D2*, *D3* are the diffusion coefficients for ammonium ($m^2\ d^{-1}$), nitrite and nitrate, δ is the thickness for one (discretized) biofilm segment (m), r_{eq} is the acid-base equilibrium reaction rate ($gN\ m^{-3}\ d^{-1}$)

Mass balances for the biofilm phase:

$$\frac{dCb_{NH3}[1..N,1]}{dt} = \frac{D1}{\delta^2} \cdot (Cl_{NH3}[1] - 2Cb_{NH3}[i,1] + Cb_{NH3}[i,2]) - rA[i,1] + r_{b\ eq,NH3}[i,1]$$

$$\frac{dCb_{NH3}[1..N,2..M-1]}{dt} = \frac{D1}{\delta^2} \cdot (Cb_{NH3}[i,j-1] - 2Cb_{NH3}[i,j] + Cb_{NH3}[i,j+1]) - rA[i,j] + r_{b\ eq,NH3}[i,j]$$

$$\frac{dCb_{NH3}[1..N,M]}{dt} = \frac{D1}{\delta^2} \cdot (Cb_{NH3}[i,j-1] - Cb_{NH3}[i,j]) - rA[i,j] + r_{b\ eq,NH3}[i,j]$$

$$\frac{dCb_{NH4}[1..N,1]}{dt} = \frac{D1}{\delta^2} \cdot (Cl_{NH4}[1] - 2Cb_{NH4}[i,1] + Cb_{NH4}[i,2]) + r_{b\ eq,NH4}[i,1]$$

$$\frac{dCb_{NH4}[1..N,2..M-1]}{dt} = \frac{D1}{\delta^2} \cdot (Cb_{NH4}[i,j-1] - 2Cb_{NH4}[i,j] + Cb_{NH4}[i,j+1]) + r_{b\ eq,NH4}[i,j]$$

$$\frac{dCb_{NH4}[1..N,M]}{dt} = \frac{D1}{\delta^2} \cdot (Cb_{NH4}[i,j-1] - Cb_{NH4}[i,j]) + r_{b\ eq,NH4}[i,j]$$

$$\frac{dCb_{NO2}[1..N,1]}{dt} = \frac{D2}{\delta^2} \cdot (Cl_{NO2}[1] - 2Cb_{NO2}[i,1] + Cb_{NO2}[i,2]) + r_{b\ eq,NO2}[i,1]$$

$$\frac{dCb_{NO2}[1..N,2..M-1]}{dt} = \frac{D2}{\delta^2} \cdot (Cb_{NO2}[i,j-1] - 2Cb_{NO2}[i,j] + Cb_{NO2}[i,j+1]) + r_{b\ eq,NO2}[i,j]$$

$$\frac{dCb_{NO2}[1..N,M]}{dt} = \frac{D2}{\delta^2} \cdot (Cb_{NO2}[i,j-1] - Cb_{NO2}[i,j]) + r_{b\ eq,NO2}[i,j]$$

$$\frac{dCb_{HNO2}[1..N,1]}{dt} = \frac{D2}{\delta^2} \cdot (Cl_{HNO2}[1] - 2Cb_{HNO2}[i,1] + Cb_{HNO2}[i,2]) + rA[i,1] - rN[i,1] + r_{b\ eq,HNO2}[i,1]$$

$$\frac{dCb_{HNO2}[1..N,2..M-1]}{dt} = \frac{D2}{\delta^2}\cdot(Cb_{HNO2}[i,j-1]-2Cb_{HNO2}[i,j]+Cb_{HNO2}[i,j+1])+rA[i,j] - rN[i,j]+r_{b\ eq,HNO2}[i,j]$$

$$\frac{dCb_{HNO2}[1..N,M]}{dt} = \frac{D2}{\delta^2}\cdot(Cb_{HNO2}[i,j-1]-Cb_{HNO2}[i,j])+rA[i,j]-rN[i,j]+r_{b\ eq,HNO2}[i,j]$$

$$\frac{dCb_{NO3}[1..N,1]}{dt} = \frac{D3}{\delta^2}\cdot(Cl_{NO3}[1]-2Cb_{NO3}[i,1]+Cb_{NO3}[i,2])+rN[i,1]+r_{b\ eq,NO3}[i,1]$$

$$\frac{dCb_{NO3}[1..N,2..M-1]}{dt} = \frac{D3}{\delta^2}\cdot(Cb_{NO3}[i,j-1]-2Cb_{NO3}[i,j]+Cb_{NO3}[i,j+1])+rN[i,j] + r_{b\ eq,NO3}[i,j]$$

$$\frac{dCb_{NO3}[1..N,M]}{dt} = \frac{D3}{\delta^2}\cdot(Cb_{NO3}[i,j-1]-Cb_{NO3}[i,j])+rN[i,j]+r_{b\ eq,NO3}[i,j]$$

Where r_A is the ammonia oxidation rate (gN m^{-3} d^{-1}), r_N is the nitrite oxidation rate (gN m^{-3} d^{-1}), rb_{eq} is the acid-base equilibrium reaction rate in biofilm (gN m^{-3} d^{-1}).

Microbial kinetics for ammonia oxidizing bacteria and nitrite oxidizing bacteria:

A Haldane model was implemented to describe the microbial kinetics for AOB and NOB. FA and FNA inhibition were included in the model following the work of Lauren (ref).

For AOB, FA was considered as substrate inhibition factor and FNA was considered as non-competitive inhibition factor. For NOB, FNA was considered as substrate inhibition factor and FA was considered as non-competitive inhibition factor. The expressions were shown as below:

$$rA[1..N, 1..M] = \mu Amax \cdot \frac{X_A}{Y_A} \cdot \frac{FA[i,j]}{K_{SA,FA} + FA[i,j] + \frac{FA[i,j]^2}{K_{IA,FA}}} \cdot \frac{K_{IA,FNA}}{K_{IA,FNA} + FNA[i,j]}$$

$$rN[1..N, 1..M] = \mu Nmax \cdot \frac{X_N}{Y_N} \cdot \frac{FNA[i,j]}{K_{SN,FNA} + FNA[i,j] + \frac{FNA[i,j]^2}{K_{SN,FNA}}} \cdot \frac{K_{IN,FA}}{K_{IN,FA} + FA[i,j]}$$

Where $\mu Amax$ and $\mu Nmax$ are the maximum specific growth rate for AOB and NOB (d^{-1}), Y_A and Y_N are the yield coefficients for AOB and NOB (g VSS/g N), $K_{SA,FA}$ and $K_{SN,FNA}$ are the half saturation coefficients for AOB and NOB (mg/L), $K_{IA,FA}$ and $K_{IA,FNA}$ are the inhibition coefficients for AOB by free ammonia and free nitrous acid (mg/L), $K_{IN,FA}$ and $K_{IN,FNA}$ are the inhibition coefficients for NOB by free ammonia and free nitrous acid (mg/L).

Acid-base equilibrium reaction:

Acid-base equilibrium reactions were included in the model to determine effect of pH on the presence of different nitrogen species. The reaction model was developed according to kinetic based model where forward and reverse reaction accounted for the equilibrium of NH_3/NH_4^+ and NO_2^-/HNO_2. The expressions are shown below:

$$r_{eq,NH3}[1..N,1..M] = k_{eq} \cdot (Cl_{NH4} - Cl_{NH3} \cdot Cl_{H^+} \cdot 10^{-PK_{NH3}})$$

$$r_{eq,NH4}[1..N,1..M] = -r_{eq,NH3}[1..N,1..M]$$

$$r_{eq,NO2}[1..N,1..M] = k_{eq} \cdot (Cl_{HNO2} - Cl_{NO2} \cdot Cl_{H^+} \cdot 10^{-PK_{NO2}})$$

$$r_{eq,HNO2}[1..N,1..M] = -r_{eq,NO2}[1..N,1..M]$$

$$r_{b\ eq,NH3}[1..N,1..M] = k_{eq} \cdot (Cb_{NH4} - Cb_{NH3} \cdot Cb_{H^+} \cdot 10^{-PK_{NH3}})$$

$$r_{b\ eq,NH4}[1..N,1..M] = -r_{b\ eq,NH3}[1..N,1..M]$$

$$r_{b\ eq,NO2}[1..N,1..M] = k_{eq} \cdot (Cb_{HNO2} - Cb_{NO2} \cdot Cb_{H^+} \cdot 10^{-PK_{NO2}})$$

$$r_{b\ eq,HNO2}[1..N,1..M] = -r_{b\ eq,HNO2}[1..N,1..M]$$

Where k_{eq} is equilibrium reaction rate (d^{-1}), *PK* is the acid dissociation constant for each nitrogen species.

Mass balance for the proton concentration:

Mass balance for the proton in liquid

$$\frac{dCl_{H^+}[1]}{dt} = \frac{F}{V_N \cdot hc} \cdot (Cl_{H^+in} - Cl_{H^+}[1]) - \frac{D4 \cdot a}{hc \cdot \delta} \cdot (Cl_{H^+}[1] - Cb_{H^+}[1,j]) + r_{eq,NO2}[1] + r_{eq,NH3}[1]$$

$$\frac{dCl_{H^+}[2..N]}{dt} = \frac{F}{V_N \cdot hc} \cdot (Cl_{H^+}[i-1] - Cl_{H^+}[i]) - \frac{D4 \cdot a}{hc \cdot \delta} \cdot (Cl_{H^+}[i] - Cb_{H^+}[i,1]) + r_{eq,NO2}[i] + r_{eq,NH3}[i]$$

Mass balance for proton in biofilm

$$\frac{dCb_{H^+}[1..N,1]}{dt} = \frac{D4}{\delta^2} \cdot (Cl_{H^+}[1] - 2Cb_{H^+}[i,1] + Cb_{H^+}[i,2]) + 2 \cdot rA[i,1] + r_{b\ eq,NH3}[i,1] + r_{b\ eq,NO2}[i,1]$$

$$\frac{dCb_{H^+}[1..N,2..M-1]}{dt} = \frac{D4}{\delta^2} \cdot (Cb_{H^+}[i,j-1] - 2Cb_{H^+}[i,j] + Cb_{H^+}[i,j+1]) + 2 \cdot rA[i,j] + r_{b\ eq,NH3}[i,j] + r_{b\ eq,NO2}[i,j]$$

$$\frac{dCb_{H^+}[1..N,M]}{dt} = \frac{D4}{\delta^2} \cdot (Cb_{H^+}[i,j-1] - Cb_{H^+}[i,j]) + 2 \cdot rA[i,j] + r_{b\ eq,NH3}[i,j] + r_{b\ eq,NO2}[i,j]$$

The mass balance for proton concentration was developed according to acid-base equilibrium reaction and nitrification process. The dissociation of NH_4^+ and HNO_2^- produced H^+. Nitrification process also produced H^+. For 1 mole of NH_4^+ consumed, 2 moles of H^+ will be produced.

3.2.2 Anammox bioreactor Model Development

Mass balance for the liquid phase:

$$\frac{dSl_{NH3}[1]}{dt} = \frac{F}{V_W} \cdot (Sl_{NH3in} - Sl_{NH3}[1]) - \frac{D1 \cdot a2}{\delta 2} \cdot (Sl_{NH3}[1] - Sb_{NH3}[1,j]) + r_{an\ eq,NH3}[1]$$

$$\frac{dSl_{NH3}[1..W]}{dt} = \frac{F}{V_W} \cdot (Sl_{NH3in} - Cl_{NH3}[i]) - \frac{D1 \cdot a2}{\delta 2} \cdot (Sl_{NH3}[i] - Sb_{NH3}[i,j]) + r_{an\ eq,NH3}[i]$$

$$\frac{dSl_{NH4}[1]}{dt} = \frac{F}{V_W} \cdot (Sl_{NH4in} - Sl_{NH4}[1]) - \frac{D1 \cdot a2}{\delta 2} \cdot (Sl_{NH4}[1] - Sb_{NH4}[1,j]) + r_{an\ eq,NH4}[1]$$

$$\frac{dSl_{NH4}[1..W]}{dt} = \frac{F}{V_W} \cdot (Sl_{NH4in} - Sl_{NH4}[i]) - \frac{D1 \cdot a2}{\delta 2} \cdot (Sl_{NH4}[i] - Sb_{NH4}[i,j]) + r_{an\ eq,NH4}[i]$$

$$\frac{dSl_{NO2}[1]}{dt} = \frac{F}{V_W} \cdot (Sl_{NO2in} - Sl_{NO2}[1]) - \frac{D2 \cdot a2}{\delta 2} \cdot (Sl_{NO2}[1] - Sb_{NO2}[1,j]) + r_{an\ eq,NO2}[1]$$

$$\frac{dSl_{NO2}[1..W]}{dt} = \frac{F}{V_W} \cdot (Sl_{NO2in} - Sl_{NO2}[i]) - \frac{D2 \cdot a2}{\delta 2} \cdot (Sl_{NO2}[i] - Sb_{NO2}[i,j]) + r_{an\ eq,NO2}[i]$$

$$\frac{dSl_{HNO2}[1]}{dt} = \frac{F}{V_W} \cdot (Sl_{HNO2in} - Sl_{HNO2}[1]) - \frac{D2 \cdot a2}{\delta 2} \cdot (Sl_{HNO2}[1] - Sb_{HNO2}[1,j]) + r_{an\ eq,HNO2}[1]$$

$$\frac{dSl_{HNO2}[1..W]}{dt} = \frac{F}{V_W} \cdot (Sl_{HNO2in} - Sl_{HNO2}[i]) - \frac{D2 \cdot a2}{\delta 2} \cdot (Sl_{HNO2}[i] - Sb_{HNO2}[i,j]) + r_{an\ eq,HNO2}[i]$$

$$\frac{dSl_{NO3}[1]}{dt} = \frac{F}{V_W} \cdot (Sl_{NO3in} - Sl_{NO3}[1]) - \frac{D3 \cdot a2}{\delta 2} \cdot (Sl_{NO3}[1] - Sb_{NO3}[1,j]) + r_{an\ eq,NO3}[1]$$

$$\frac{dSl_{NO3}[1..W]}{dt} = \frac{F}{V_W} \cdot (Sl_{NO3in} - Sl_{NO3}[i]) - \frac{D3 \cdot a2}{\delta 2} \cdot (Sl_{NO3}[i] - Sb_{NO3}[i,j]) + r_{an\ eq,NO3}[i]$$

Where F is the flow rate of liquid ($m^3\ d^{-1}$), $D1$, $D2$, $D3$ are the diffusion coefficients for ammonium ($m^2\ d^{-1}$), nitrite and nitrate, $\delta 2$ is the thickness for one (discretized) biofilm segment (m), $r_{an\ eq}$ is the acid-base equilibrium reaction rate ($gN\ m^{-3}\ d^{-1}$), a2 is the specific

biofilm surface area for Anammox bacteria (m^{-1}), V_w is the volume for one individual (discretized) horizontal layer (m^3).

Mass balance for biofilm phase:

$$\frac{dSb_{NH3}[1..W,1]}{dt} = \frac{D1}{\delta 2^2} \cdot (Sl_{NH3}[1] - 2Sb_{NH3}[i,1] + Sb_{NH3}[i,2]) + r_{anb\ eq,NH3}[i,1]$$

$$\frac{dSb_{NH3}[1..W,2..P-1]}{dt} = \frac{D1}{\delta 2^2} \cdot (Sb_{NH3}[i,j-1] - 2Sb_{NH3}[i,j] + Sb_{NH3}[i,j+1]) + r_{anb\ eq,NH3}[i,j]$$

$$\frac{dSb_{NH3}[1..W,P]}{dt} = \frac{D1}{\delta 2^2} \cdot (Sb_{NH3}[i,j-1] - Sb_{NH3}[i,j]) + r_{anb\ eq,NH3}[i,j]$$

$$\frac{dSb_{NH4}[1..W,1]}{dt} = \frac{D1}{\delta 2^2} \cdot (Sl_{NH4}[1] - 2Sb_{NH4}[i,1] + Sb_{NH4}[i,2]) + r_{anb\ eq,NH4}[i,1] - r1[i,1]$$

$$\frac{dSb_{NH4}[1..W,2..P-1]}{dt} = \frac{D1}{\delta 2^2} \cdot (Sb_{NH4}[i,j-1] - 2Sb_{NH4}[i,j] + Sb_{NH4}[i,j+1]) + r_{anb\ eq,NH4}[i,j] - r1[i,j]$$

$$\frac{dSb_{NH4}[1..W,P]}{dt} = \frac{D1}{\delta 2^2} \cdot (Sb_{NH4}[i,j-1] - Sb_{NH4}[i,j]) + r_{anb\ eq,NH4}[i,j] - r1[i,j]$$

$$\frac{dSb_{NO2}[1..W,1]}{dt} = \frac{D2}{\delta 2^2} \cdot (Sl_{NO2}[1] - 2Sb_{NO2}[i,1] + Sb_{NO2}[i,2]) + r_{anb\ eq,NO2}[i,1] - r2[i,1]$$

$$\frac{dSb_{NO2}[1..W,2..P-1]}{dt}$$

$$= \frac{D2}{\delta 2^2} \cdot (Sb_{NO2}[i,j-1] - 2Sb_{NO2}[i,j] + Sb_{NO2}[i,j+1]) + r_{anb\ eq,NO2}[i,j]$$

$$- r2[i,j]$$

$$\frac{dSb_{NO2}[1..W,P]}{dt} = \frac{D2}{\delta 2^2} \cdot (Sb_{NO2}[i,j-1] - Sb_{NO2}[i,j]) + r_{anb\ eq,NO2}[i,j] - r2[i,j]$$

$$\frac{dSb_{HNO2}[1..W,1]}{dt} = \frac{D2}{\delta 2^2} \cdot (Sl_{HNO2}[1] - 2Sb_{HNO2}[i,1] + Sb_{HNO2}[i,2]) + r_{anb\ eq,HNO2}[i,1]$$

$$\frac{dSb_{HNO2}[1..W,2..P-1]}{dt}$$

$$= \frac{D2}{\delta 2^2} \cdot (Sb_{HNO2}[i,j-1] - 2Sb_{HNO2}[i,j] + Sb_{HNO2}[i,j+1])$$

$$+ r_{anb\ eq,HNO2}[i,j]$$

$$\frac{dSb_{HNO2}[1..W,P]}{dt} = \frac{D2}{\delta 2^2} \cdot (Sb_{HNO2}[i,j-1] - Sb_{HNO2}[i,j]) + r_{anb\ eq,HNO2}[i,j]$$

$$\frac{dSb_{NO3}[1..W,1]}{dt} = \frac{D3}{\delta 2^2} \cdot (Sl_{NO3}[1] - 2Sb_{NO3}[i,1] + Sb_{NO3}[i,2]) + r3[i,1] + r_{anb\ eq,NO3}[i,1]$$

$$\frac{dSb_{NO3}[1..W,2..P-1]}{dt}$$

$$= \frac{D3}{\delta 2^2} \cdot (Sb_{NO3}[i,j-1] - 2Sb_{NO3}[i,j] + Sb_{NO3}[i,j+1]) + r3[i,j]$$

$$+ r_{anb\ eq,NO3}[i,j]$$

$$\frac{dSb_{NO3}[1..W,P]}{dt} = \frac{D3}{\delta 2^2} \cdot (Sb_{NO3}[i,j-1] - Sb_{NO3}[i,j]) + r3[i,j] + r_{anb\ eq,NO3}[i,j]$$

Where *r1* is the ammonia consumption rate (gN m^{-3} d^{-1}), *r2* is the nitrite consumption rate (gN m^{-3} d^{-1}), *r3* is the nitrate production rate (gN m^{-3} d^{-1}). $r_{anb\ eq}$ is the acid-base equilibrium reaction rate in biofilm (gN m^{-3} d^{-1}).

Microbial kinetics for Anammox bacteria:

The microbial kinetic for Anammox bacteria was described by a Monod-Haldane model. Inhibition factor by nitrite was included in the model consistent with the work of Pradhan et al. (2020). However, inhibitory effect by ammonium was ignored due to the fact that Anammox bacteria was more sensitive to FNA inhibition than FA inhibition. Indeed, the result from experimental study also demonstrated this point. The general expression of Anammox kinetic model is shown below:

$$r1[1..W,1..P] = \mu ANmax \cdot \frac{X_{AN}}{Y_{AN}} \cdot \frac{Sb_{NO2}[i,j]}{K_{SAN,NO2} + Sb_{NO2}[i,j] + \frac{Sb_{NO2}[i,j]^2}{K_{IAN,NO2}}} \cdot \frac{Sb_{NH4}[i,j]}{K_{SAN,FNA} + Sb_{NH4}[i,j]}$$

$$r2[1..W,1..P] = 1.32 \cdot r1[1..N,1..M]$$

$$r3[1..W,1..P] = 0.26 \cdot r1[1..N,1..M]$$

Where $\mu ANmax$ is the maximum specific growth rate for Anammox bacteria (d^{-1}), Y_{AN} is the yield coefficients for Anammox bacteria (g COD/g N), $K_{SAN,NO2}$ and $K_{SAN,\ NH4}$ are the

half saturation coefficients for Anammox bacteria (mg/L), $K_{IAN,NO2}$ is the inhibition coefficients for Anammox bacteria by nitrite (mg/L). The rates of nitrite consumption and nitrate production were described based on the stoichiometric ratio of Anammox reaction.

Acid-base equilibrium reactions:

The acid-base equilibrium reactions for Anammox bioreactor were very similar to those of nitrification process in BTF. Therefore, the expressions for these reactions are not repeated in the text.

3.3 Model Simulation

For model simulation, the operating parameters such as gas flow rate, liquid flow rate and reactor size were set to those values used in the laboratory. Microbial kinetic parameters and parameters for physical-chemical properties such as diffusion coefficient, mass transfer coefficient and acid-base equilibrium constant were adopted from existing literature. Other parameters such as biofilm thickness, hydraulic holdup, porosity and biomass densities were calculated according to the results of actual experiments. The performance of BTF coupled with Anammox bioreactor was simulated based on variations of nitrogen species in liquid phase. For the purpose of optimizing the integrated system, the effect of different operating parameters on system performance was also investigated through parameter plots.

3.3.1 Overall performance of Coupled System

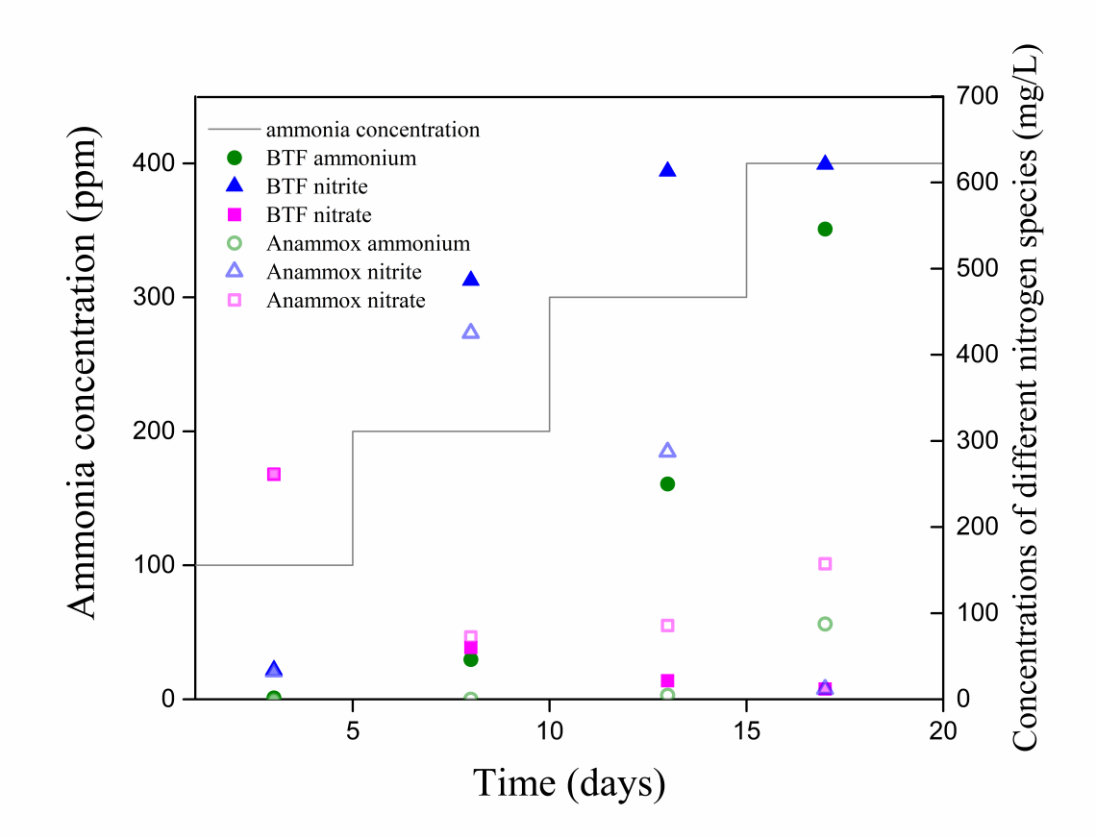

Figure 7: Simulated Overall Performance of Coupled System with Different Inlet Ammonia Concentration

Fig. 7 shows the overall simulated performance of the integrated system with ammonia concentration ranging from 100 – 400 ppm. The air flow rate was constant which means the ammonia nitrogen loading was proportional to inlet ammonia concentration. When the inlet ammonia concentration was 100 ppm, nearly all ammonia dissolved in liquid phase and was converted to nitrate and no significant accumulation of nitrite was observed. This indicates that full nitrification was achieved under low ammonia loading condition because low concentrations of metabolites did not inhibit

activity of NOB. When ammonia concentration was gradually increased, the concentration of nitrite in the BTF effluent increased significantly which caused the activity of NOB to be suppressed at medium and high nitrogen loading. When inlet ammonia concentrations were 300 ppm and 400 ppm, the ammonium conversion ratio ($(NO_3^-$-N+NO_2^--N)/NH_4^+-N) became lower which indicated activity of AOB was also partially inhibited.

The Anammox bioreactor was connected to the BTF in the simulation. When the inlet ammonia concentration was 100 ppm, full nitrification was achieved and only small amount of nitrite and ammonium was produced. At this ammonia concentration, conventional denitrification reactor would thus be more suitable than Anammox reactor for post treatment. When concentrations of ammonia were 200 ppm and 300 ppm, nitrite concentration were much higher than ammonium BTF effluent due to the reason that AOB was not inhibited in those conditions. Therefore, the ratio of NO_2^--N /NH_4^+-N was larger than stoichiometric ratio of Anammox reaction. Excess ammonium was predicted to remain in the Anammox effluent because of relative deficiency of ammonium in influent. When inlet ammonia concentration increased to 400 ppm, concentration of ammonium in the BTF effluent also increased because activity of AOB began to get inhibited by metabolites. The ration of NO_2^--N /NH_4^+-N decreased and excess ammonium was predicted in the Anammox effluent.

The results of these simulations show that a proper ratio of NO_2^--N /NH_4^+-N (1.32) is essential to achieve complete nitrogen elimination in this system. High concentrations of metabolites will inhibit the activity of AOB and NOB. Because these metabolites (FA and FNA) served as both substrates and inhibitors for microbial growth, it was important to understand factors that may influence the presence of these metabolites in the system to optimize system performance.

3.3.2 Ammonia Gas Removal in Biotrickling Filter

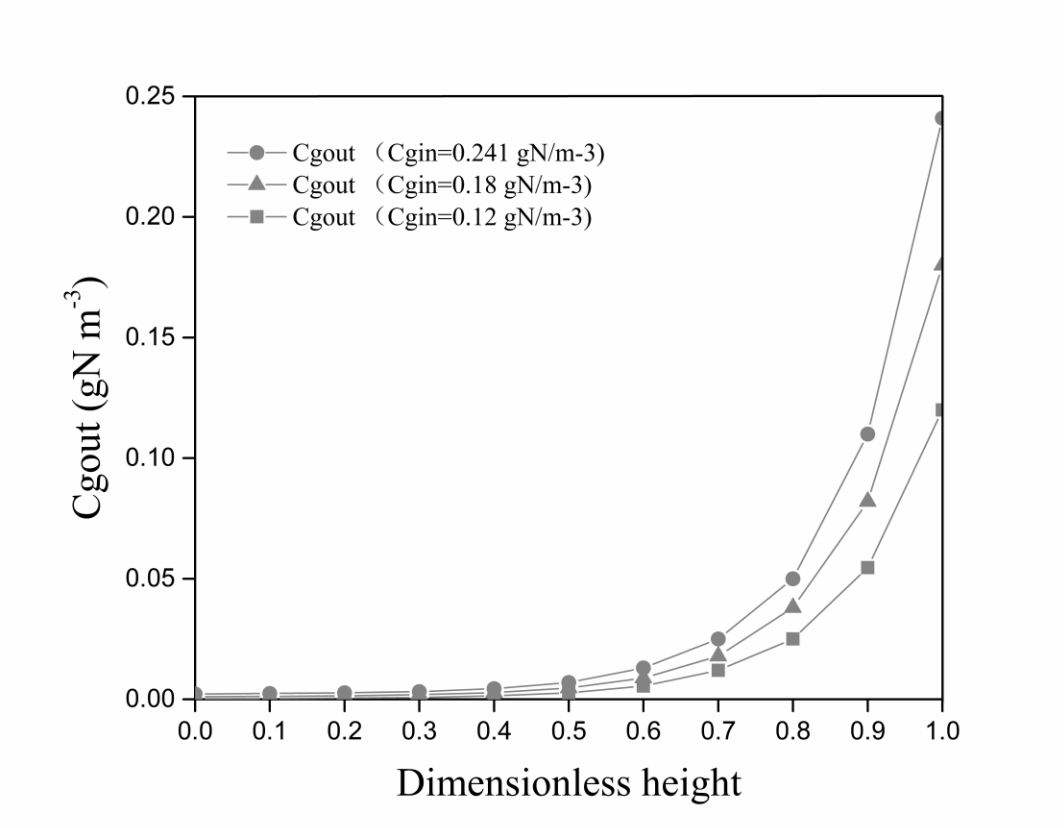

Figure 8: Simulated Ammonia Gas Concentration along the Bed Height with Different Inlet Concentrations

Fig. 8 reports the model simulated performance of BTF in gas phase with different inlet ammonia concentrations. The results showed at an EBRT of 20.8 s with different inlet ammonia concentrations, most of ammonia gas should be removed in the upper part of the reactor. This was probably due to a high ammonia mass transfer coefficient selected in this study which means mass transfer was not a limiting step for this study. At the highest ammonia concentration (400 ppm), 90% removal of ammonia was achieved in only 30% of the total reactor height. While for the lowest ammonia concentration (200 ppm), 50% of the total reactor height was needed to remove 90% of ammonia in the gas. A higher inlet ammonia concentration will enhance the gas-liquid mass transfer. However, if high concentration of ammonia caused severe inhibition on microbial activity, ammonia removal performance will get deteriorated.

3.3.3 Impact of Different Parameters on Biotrickling Filter Performance

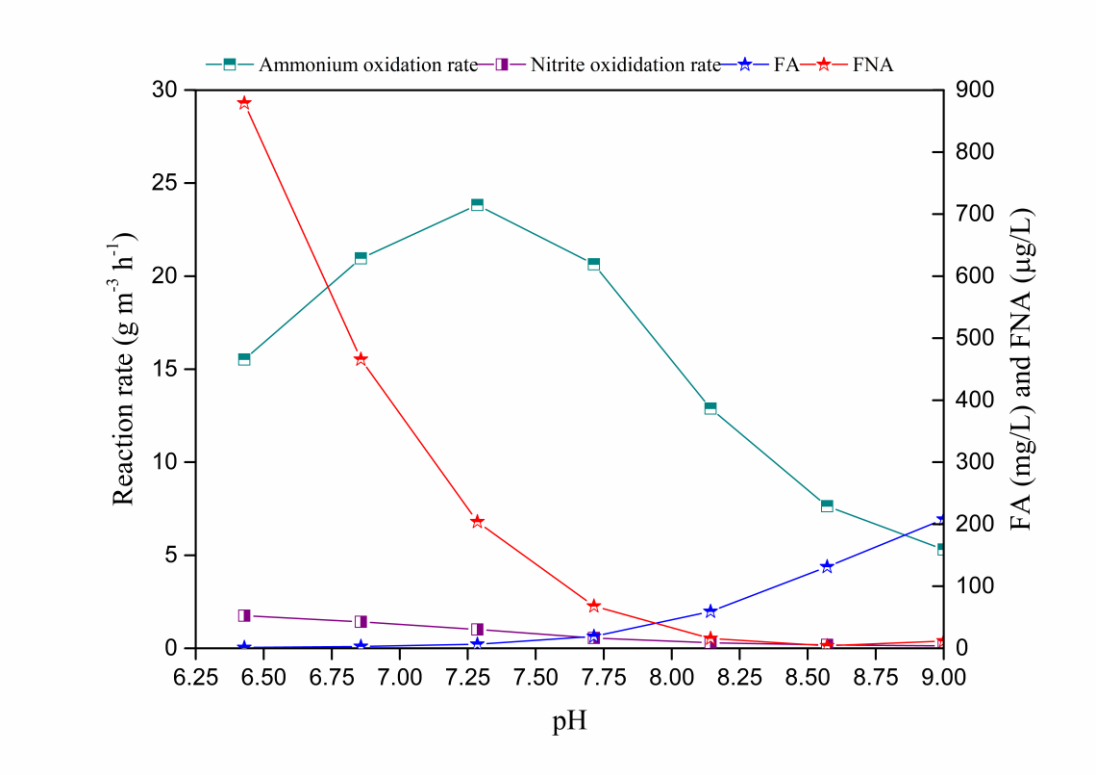

Figure 9: Effect of pH on Microbial Activities and Variations of Metabolites

Fig. 9 shows the model simulated effects of pH on the ammonium oxidation rates and nitrite oxidation rates which represented activities for AOB and NOB respectively. At pH ranged from 7 – 7.5, the activity of AOB was the highest due to both relative low concentration of FA and FNA. At pH outside this range, either high concentrations of FA and FNA inhibited AOB activity. Moreover, the relative low pH condition was not suitable for the presence of FA in liquid which also was the actual substrate for AOB. Thus, significant decrease of ammonium oxidation rate was observed when pH was below 6.8 or above 7.75. The nitrite oxidation rate decreased with

increasing pH, this is probably because at high pH conditions, the concentration of FNA decreased significantly which severed as the actual substrate for NOB activity.

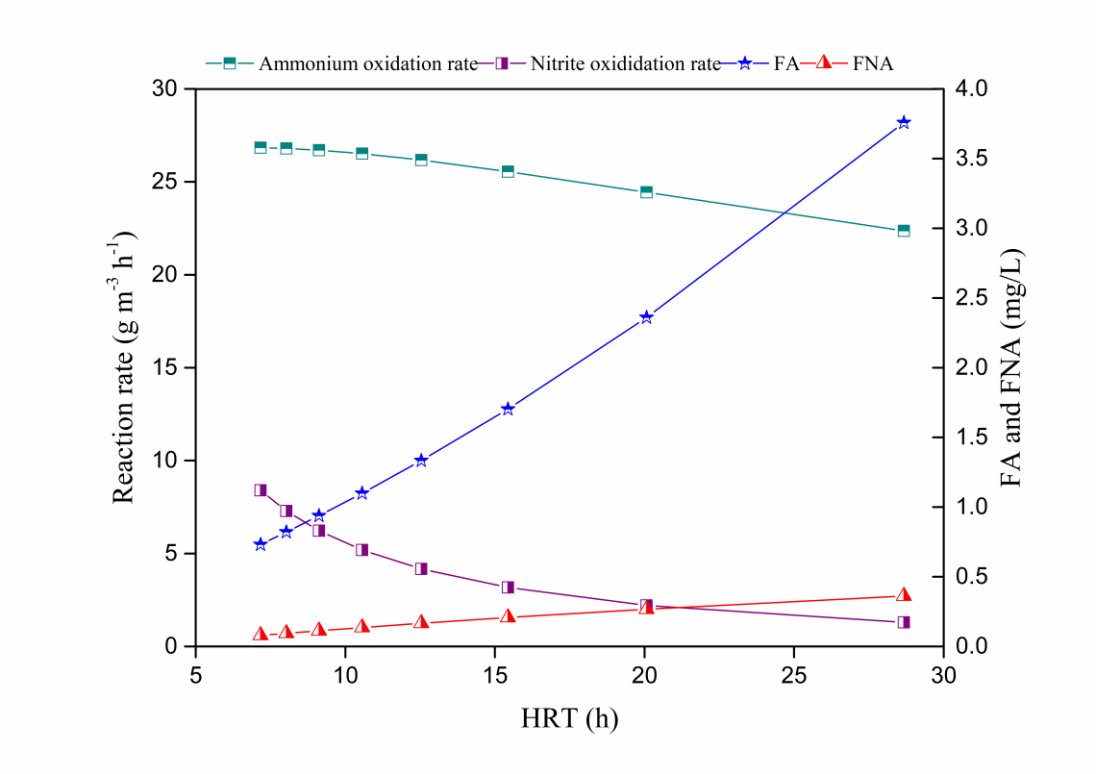

Figure 10: Effect of HRT on Microbial Activities and Variations of Metabolites

As shown in Fig. 10, with increasing HRT, both activities of AOB and NOB were inhibited as a result of increasing concentrations of FA and FNA. Compared to the ammonium oxidation rate, the large decrease of nitrite oxidation rates indicated that NOB was more vulnerable to inhibition than AOB. The simulated results suggested that shortening hydraulic residence time was an effective way to achieve partial nitritation in BTF by increasing the concentration of substrates. On the contrary, a higher flow rate was essential to avoid inhibitory effect on microbial activities to achieve full nitrification.

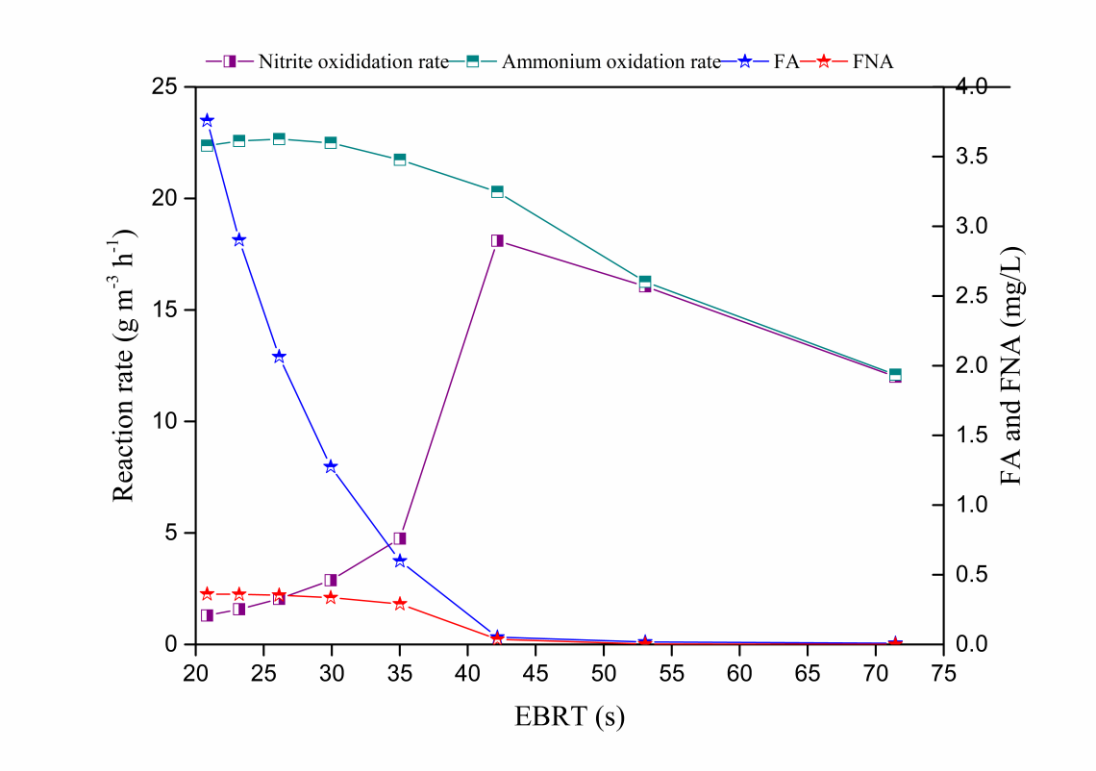

Figure 11: Effect of EBRT on Microbial Activities and Variations of Metabolites

In Fig. 11, the simulation was conducted at a constant inlet ammonia concentration of 400 ppm. Thus, EBRT was inversely correlated with nitrogen loading rate (NLR). Hence, with increasing EBRT (lower gas flow rate), NLR was reduced which led to lower concentration of FA and FNA in BTF. However, the ammonium oxidation rate significantly decreased with increasing EBRT. This was probably because that increasing EBRT made less ammonia available for AOB activity (i.e., a lower loading). Nitrite oxidation rate was improved with increasing EBRT initially. However, when both concentrations of FA and FNA were low at EBRT higher than 40s, substrate

limitation was the main factor that impacted microbial activity. It is worth mentioning that at EBRT higher than 53 s., nitrite oxidation rate was equal to ammonium oxidation rate which indicated that full nitrification was achieved.

Based on the results obtained from Fig. 8, 9 and 10, operating parameters of BTF had very large impact on the performance of the system and concentrations of N species in liquid phase. If mass transfer process of ammonia was not the limiting step, biological reaction would have influenced the ratio of different nitrogen species in liquid phase which may have an subsequent impact on denitrification process. Proper ratio of different nitrogen species could be achieved through the regulation of HRT and EBRT. pH was also an important factor as it influenced the presence of FA and FNA. It should be noted that simulations conducted above were based on a constant proton concentration. Whereas in the real situation, pH was also a variable that may be impacted by other operating parameters. To account for the dynamic change of pH as a result of the absorption of ammonia and nitrification process, mass balance for proton concentration was included and pH was also simulated. The result was shown in Fig. 12.

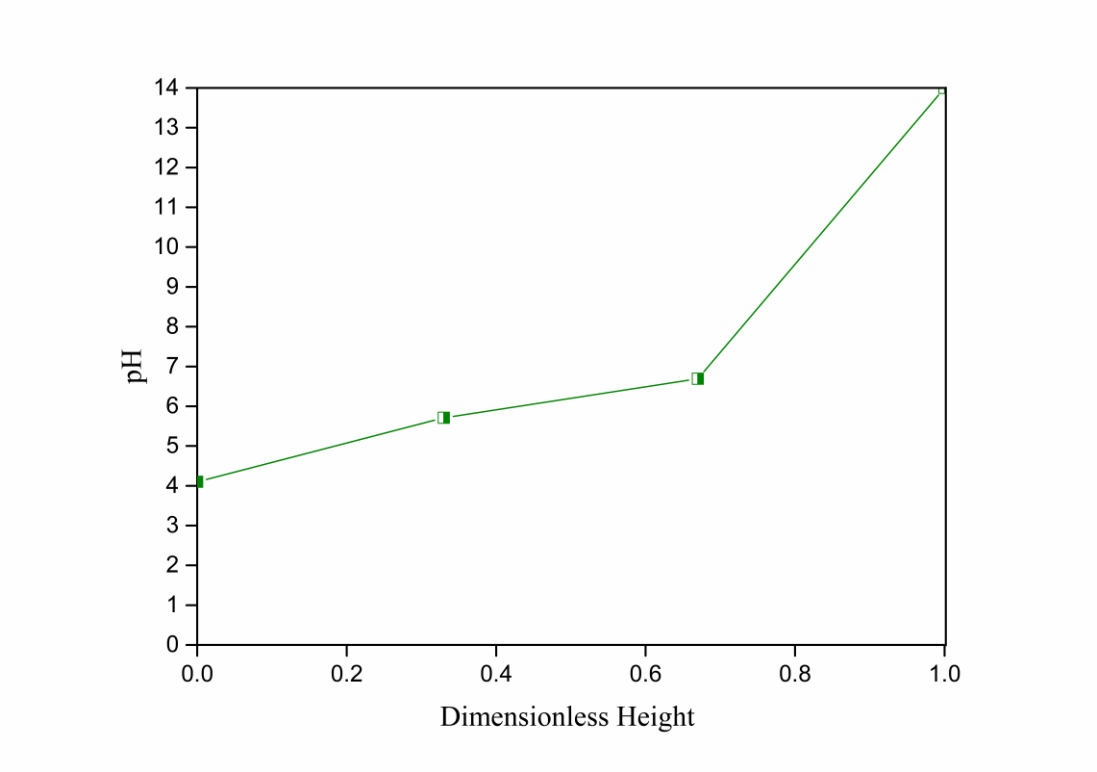

Figure 12: Change of pH along Bed Height

Due to the nitrification process, pH gradually decreased along the bed height. The BTF effluent pH decreased to 4.1 with an influent pH of 7. However, this value was not consistent with actual experimental data. According to the experimental data, BTF effluent pH never dropped below 6. Sakuma et al. (2004) and Baquerizo et al. (2007) also predicted pH of biofilter and biotrickling filter within the range of 3 to 5 using kinetic based model. Baquerizo et al. (2007) stated that acid-base equilibrium of other species such as carbonate species should be also included to accurately predict pH. Thus, the

dramatic drop of pH in this model was probably because that buffer capacity of other substances in mineral medium was not considered. This buffering should be added next.

3.3.4 Impact of Recycle on Anammox Performance

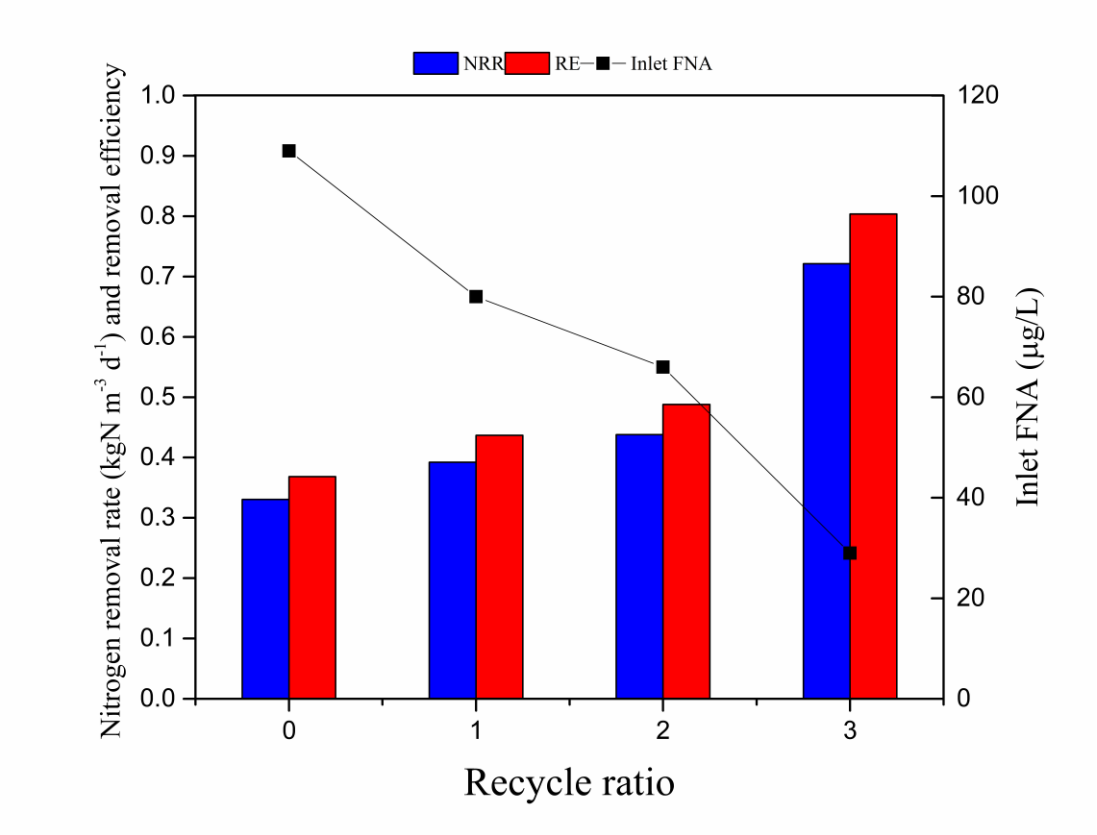

Figure 13: Nitrogen Removal Rate and Efficiency with Different Recycle Ratio

Anammox activity could be easily inhibited due to accumulation of metabolites, especially nitrite according to the result obtained from laboratory studies reported in this thesis. A proper recycle of the Anammox effluent to the inlet of the Anammox reactor can be implemented to reduce the inhibitory effect of nitrite by diluting inlet concentration. Fig. 13 shows that at constant nitrogen loading, the nitrogen removal

efficiency could be greatly enhanced with a higher recycle ratio. Inlet FNA concentration was reduced 4 times lower than that without recycle. To connect Anammox bioreactor with BTF, it was of great importance to have a recycle to dilute the inlet concentration because high concentration of FNA was maintained in the BTF to constantly suppress NOB whereas Anammox bacteria may also get inhibited at such high concentration of FNA.

4. Conclusion

With ammonia concentration of 400 ppm_v and inlet nitrogen loading rate of 50 $gN\ m^{-3}\ h^{-1}$, ideal nitritation in BTF was achieved and the average ammonia removal efficiency was 95% for long term operation. The BTF-Anammox bioreactor coupled system was realized under one pass mode. Average nitrogen removal efficiency and nitrogen removal rate were 76.8% and 0.64 $kgN\ m^{-3}\ d^{-1}$ respectively. Recycle from Anammox to BTF did not have a large impact on the performance of BTF but significantly weakened the performance of Anammox due to accumulation of nitrite in the system. To successfully achieve complete and long-term closed loop mode, Anammox activity should be further enhanced by optimizing operation condition or enlarging reactor size.

The model developed for biotrickling filter-Anammox bioreactor integrated system could successfully describe the process of shortcut nitrification under medium and high conditions. Impact of different parameters on the performance of biotrickling filter and Anammox bioreactor were investigated through parametric sensitivity studies. EBRT strongly influence the activity of both AOB and NOB. Increasing recycle ratio of Anammox bioreactor can increase nitrogen removal rate of Anammox bioreactor through reducing inhibitory effect by high concentration of FNA.

Further Improvement of Model

(1) Using kinetic based model and just proton and N species did not describe dynamic change of pH condition along the reactor appropriately according to actual experimental data. Acid-base equilibrium for other chemicals especially buffer substances in mineral medium should also be included in the model.

(2) Microbial kinetic parameters in the model were obtained from literature. The kinetic characteristics for my system may be different from others due to different operating conditions and extent of acclimation of sludge to the specific condition. Experimental batch tests areneeded to determine kinetic parameters for the specific system being modeled.

(3) Biomass densities within biofilm needs to be determined by experiment. In this model, uniform biomass densities were assumed along the height of reactors. However, biomass densities in real situation may be variable along the height.

Appendix A

Table 2: Model Parameters.

Parameter	Symbol	Units	Value	Reference
BTF				
Maximum growth rate of AOB	μA_{max}	day^{-1}	1.21	Jubany et al
Half saturation coefficient for free ammonia	$Ks_{A,FA}$	mg/L	0.34	Jubany et al
Inhibition coefficient of AOB for FA	$K_{IA,FA}$	mg/L	27	Park et al
Inhibition coefficient of AOB for FNA	$K_{IA,FNA}$	mg/L	0.59	Carrera et al
Maximum growth rate of NOB	μN_{max}	day-1	1.02	Jubany et al
Half saturation coefficient for free nitrous acid	$Ks_{N,FNA}$	mg/L	$8*10^{-3}$	Jubany et al
Inhibition coefficient of NOB for FA	$K_{IN,FA}$	mg/L	0.52	Carrera et al
Inhibition coefficient of NOB for FNA	$K_{IN,FNA}$	mg/L	0.065	Carrera et al
Yield coefficient for AOB	Y_A	g VSS/g N	0.127	Jubany et al
Yield coefficient for NOB	Y_N	g VSS/g N	0.056	Jubany et al
Diffusion coefficient for total ammonia	D1	m2/d	$119.28*10^{-6}$	Baquerizo et al
Diffusion coefficient for total nitrite	D2	m2/d	$106.32*10^{-6}$	Baquerizo et al

Diffusion coefficient for total nitrate	D3	m2/d	$106.32*10^{-6}$	Baquerizo et al
Gas-liquid mass transfer coefficient for ammonia	k_g	m/d	480	Lauren
Porosity of the filter bed	e	/	0.8	Lauren
Dynamic hold-up	hc	/	0.1	Adjusted by simulation
Biofilm surface area	s	m^2	1.79	Lauren
Biofilm thickness	δ	M	$1*10^{-4}$	Lauren
Anammox Bioreactor				
Maximum specific growth rate	μAN_{max}	day^{-1}	0.0984	Oshiki et al
Half saturation coefficient for ammonium	$Ks_{AN,NH4}$	mg/L	0.39	Oshiki et al
Half saturation coefficient for nitrite	$Ks_{AN,NO2}$	mg/L	1.39	Oshiki et al
Inhibition coefficient of anammox for nitrite	$K_{IAN,NO2}$	mg/L	210	Oshiki et al
Biofilm surface area	S_1	m2	0.49	Lauren
Biofilm thickness	δ_2	M	$3*10^{-4}$	Lauren
Yield coefficient	Y_{AN}	g COD/ g N	0.067	Strous et al

References

Anthonisen, A. C., Loehr, R. C., Prakasam, T., & Srinath, E. (1976). Inhibition of nitrification by ammonia and nitrous acid. *Journal (Water Pollution Control Federation)*, 835-852.

Baquerizo, G., Gamisans, X., Gabriel, D., & Lafuente, J. (2007). A dynamic model for ammonia abatement by gas-phase biofiltration including pH and leachate modelling. *Biosystems engineering, 97*(4), 431-440.

Baquerizo, G., Maestre, J. P., Sakuma, T., Deshusses, M. A., Gamisans, X., Gabriel, D., & Lafuente, J. (2005). A detailed model of a biofilter for ammonia removal: model parameters analysis and model validation. *Chemical engineering journal, 113*(2-3), 205-214.

Behera, S. N., Sharma, M., Aneja, V. P., & Balasubramanian, R. (2013). Ammonia in the atmosphere: a review on emission sources, atmospheric chemistry and deposition on terrestrial bodies. *Environmental Science and Pollution Research, 20*(11), 8092-8131.

Blázquez, E., Bezerra, T., Lafuente, J., & Gabriel, D. (2017). Performance, limitations and microbial diversity of a biotrickling filter for the treatment of high loads of ammonia. *Chemical Engineering Journal, 311*, 91-99.

Carfrae, J., Sheppard, L., Raven, J., Leith, I., Stein, W., Crossley, A., & Theobald, M. (2004). Early effects of atmospheric ammonia deposition on Calluna vulgaris (L.) hull growing on an ombrotrophic peat bog. *Water, Air, & Soil Pollution: Focus, 4*(6), 229-239.

Carrera, J. (2000) *Biological nutrient removal from high-strength wastewater: analysis of process parameters and design of a full-scale wastewater treatment plant, Ph.D. Thesis*, Universitat Autònoma de Barcelona Ed. (in Spanish)

Dapena-Mora, A., Fernandez, I., Campos, J., Mosquera-Corral, A., Mendez, R., & Jetten, M. (2007). Evaluation of activity and inhibition effects on Anammox process by batch tests based on the nitrogen gas production. *Enzyme and Microbial Technology, 40*(4), 859-865.

Deshusses, M. A. (2005). Application of immobilised cells for air pollution control. In *Applications of Cell Immobilisation Biotechnology* (pp. 507-526): Springer.

Egli, K., Fanger, U., Alvarez, P. J., Siegrist, H., van der Meer, J. R., & Zehnder, A. J. (2001). Enrichment and characterization of an anammox bacterium from a rotating biological contactor treating ammonium-rich leachate. *Archives of microbiology, 175*(3), 198-207.

Fernández, I., Dosta, J., Fajardo, C., Campos, J., Mosquera-Corral, A., & Méndez, R. (2012). Short-and long-term effects of ammonium and nitrite on the Anammox process. *Journal of Environmental Management, 95*, S170-S174.

Gut, L., Płaza, E., Trela, J., Hultman, B., & Bosander, J. (2006). Combined partial nitritation/Anammox system for treatment of digester supernatant. *Water science and technology, 53*(12), 149-159.

He, S., Chen, Y., Qin, M., Mao, Z., Yuan, L., Niu, Q., & Tan, X. (2018). Effects of temperature on anammox performance and community structure. *Bioresource technology, 260*, 186-195.

Hellinga, C., Van Loosdrecht, M., & Heijnen, J. (1999). Model based design of a novel process for nitrogen removal from concentrated flows. *Mathematical and computer modelling of dynamical systems, 5*(4), 351-371.

Hu, B., Zheng, P., Li, J., Xu, X., & Jin, R. (2006). Identification of a denitrifying bacterium and verification of its anaerobic ammonium oxidation ability. *Science in China Series C: Life Sciences, 49*(5), 460-466.

Isaka, K., Sumino, T., & Tsuneda, S. (2007). High nitrogen removal performance at moderately low temperature utilizing anaerobic ammonium oxidation reactions. *Journal of bioscience and bioengineering, 103*(5), 486-490.

Jin, R.-C., Yang, G.-F., Yu, J.-J., & Zheng, P. (2012). The inhibition of the Anammox process: a review. *Chemical engineering journal, 197*, 67-79.

Jubany Güell, I. (2007). *Operation, modeling and automatic control of complete and partial nitrification of highly concentrated ammonium wastewater*: Universitat Autònoma de Barcelona.

Kennes, C., & Veiga, M. C. (2013). *Bioreactors for waste gas treatment* (Vol. 4): Springer Science & Business Media.

Lackner, S., Gilbert, E. M., Vlaeminck, S. E., Joss, A., Horn, H., & van Loosdrecht, M. C. (2014). Full-scale partial nitritation/anammox experiences–an application survey. *Water research, 55*, 292-303.

Li, B., & Irvin, S. (2007). The comparison of alkalinity and ORP as indicators for nitrification and denitrification in a sequencing batch reactor (SBR). *Biochemical Engineering Journal, 34*(3), 248-255.

Marina, C., Kunz, A., Bortoli, M., Scussiato, L. A., Coldebella, A., Vanotti, M., & Soares, H. M. (2016). Kinetic models for nitrogen inhibition in ANAMMOX and nitrification process on deammonification system at room temperature. *Bioresource technology, 202*, 33-41.

Mulder, A., Van de Graaf, A. A., Robertson, L., & Kuenen, J. (1995). Anaerobic ammonium oxidation discovered in a denitrifying fluidized bed reactor. *FEMS microbiology ecology, 16*(3), 177-183.

Oshiki, M., Shimokawa, M., Fujii, N., Satoh, H., & Okabe, S. (2011). Physiological characteristics of the anaerobic ammonium-oxidizing bacterium 'Candidatus Brocadia sinica'. *Microbiology, 157*(6), 1706-1713.

Park, S., & Bae, W. (2009). Modeling kinetics of ammonium oxidation and nitrite oxidation under simultaneous inhibition by free ammonia and free nitrous acid. *Process Biochemistry, 44*(6), 631-640.

Pradhan, N., Thi, S. S., & Wuertz, S. (2019). Inhibition factors and kinetic model for anaerobic ammonia oxidation in a granular sludge bioreactor with Candidatus Brocadia. *Chemical engineering journal*, 123618.

Prakasam, T., & Loehr, R. (1972). Microbial nitrification and denitrification in concentrated wastes. *Water Research, 6*(7), 859-869.

Sakuma, T., Aoki, M., Hattori, T., Gabriel, D., & Deshusses, M. (2004). *A conceptual model for the treatment of ammonia vapors in a biotrickling filter.* Paper presented at the Annual Meeting and Exhibition of the Air and Waste Management Association, Pittsburgh, PA. Indianapolis, IN.

Sakuma, T., Jinsiriwanit, S., Hattori, T., & Deshusses, M. A. (2008). Removal of ammonia from contaminated air in a biotrickling filter–denitrifying bioreactor combination system. *Water Research, 42*(17), 4507-4513.

Smith, V. H., Tilman, G. D., & Nekola, J. C. (1999). Eutrophication: impacts of excess nutrient inputs on freshwater, marine, and terrestrial ecosystems. *Environmental pollution, 100*(1-3), 179-196.

Strous, M., Heijnen, J., Kuenen, J. G., & Jetten, M. (1998). The sequencing batch reactor as a powerful tool for the study of slowly growing anaerobic ammonium-oxidizing microorganisms. *Applied microbiology and biotechnology, 50*(5), 589-596.

Tang, C.-J., Zheng, P., Chai, L.-Y., & Min, X.-B. (2013). Thermodynamic and kinetic investigation of anaerobic bioprocesses on ANAMMOX under high organic conditions. *Chemical engineering journal, 230*, 149-157.

Tang, C.-j., Zheng, P., Mahmood, Q., & Chen, J.-w. (2010). Effect of substrate concentration on stability of anammox biofilm reactors. *Journal of Central South University of Technology, 17*(1), 79-84.

Tsushima, I., Ogasawara, Y., Kindaichi, T., Satoh, H., & Okabe, S. (2007). Development of high-rate anaerobic ammonium-oxidizing (anammox) biofilm reactors. *Water Research, 41*(8), 1623-1634.

Vadivelu, V., Keller, J., & Yuan, Z. (2007). Free ammonia and free nitrous acid inhibition on the anabolic and catabolic processes of Nitrosomonas and Nitrobacter. *Water science and technology, 56*(7), 89-97.

Vadivelu, V. M., Yuan, Z., Fux, C., & Keller, J. (2006). The inhibitory effects of free nitrous acid on the energy generation and growth processes of an enriched Nitrobacter culture. *Environmental science & technology, 40*(14), 4442-4448.

Wang, Z., Peng, Y., Miao, L., Cao, T., Zhang, F., Wang, S., & Han, J. (2016). Continuous-flow combined process of nitritation and ANAMMOX for treatment of landfill leachate. *Bioresource technology, 214*, 514-519.